Analytical and numerical studies of fluid reservoirs and fracture development in heterogeneous rocks

Dissertation for the degree of Philosophiae Doctor (PhD)

Ingrid Fjeldskaar Løtveit

Department of Earth Science
University of Bergen

2009

Preface

This is my dissertation submitted as a partial fulfillment of the requirements for the degree of Philosophiae Doctor in Geology at the Faculty of Mathematics and Natural Sciences, University of Bergen. The majority of the work has been carried out as a doctor student at the Department of Earth Science during November 2001 to August 2005, and more recently as an employee at International Research Institute of Stavanger (IRIS). Professor Agust Gudmundsson has been the supervisor for this project, and the main funding has been provided by the Research Council of Norway. The last part of the project has been supported by the Research Council of Norway and StatoilHydro.

Outline

The thesis consists of two parts. The first part includes an introduction to the work, with brief reviews of related topics and summaries of the papers. The second part contains six research papers. Four of the papers are published in international scientific journals, the last two are submitted or to be submitted.

The following research papers are included in the second part of the thesis:

Paper A: Propagation pathways and fluid transport of hydrofractures in jointed and layered rocks in geothermal fields. Gudmundsson, A., Fjeldskaar, I. and Brenner, S. L., 2002. *Journal of Volcanology and Geothermal Research 116, 257-278.*

Paper B: Fracture-generated permeability and groundwater yield in Norway. Gudmundsson, A., Fjeldskaar, I. and Gjesdal, O., 2002. *NGU Bulletin 439, 61-69.*

Paper C: Effects of linking up of discontinuities on fracture growth and groundwater transport. Gudmundsson, A., Gjesdal, O., Brenner, S. L. and Fjeldskaar, I., 2003. *Hydrogeology Journal 11, 84-99.*

Paper D: Dyke emplacement in a layered and faulted rift zone. Gudmundsson, A. and Loetveit, I. F., 2005. *Journal of Volcanology and Geothermal Research Special Issue 144, 311-327.*

Paper E: Propagation, deflection, arrest, and shape of hydrofractures in heterogeneous rocks. Løtveit, I. F., Gudmundsson, A. and Philipp S. L. *To be submitted.*

Paper F: Effects of glacial erosion on the state of stress and fluid pressure in petroleum reservoirs in the Barents Sea. Løtveit, I. F., Gudmundsson, A., Leknes, L., Riis, F. and Fjeldskaar, W. *Submitted to Journal of the Geological Society.*

Parts of the results of this thesis were presented as the following talks and posters:

Løtveit, I. F., Gudmundsson, A., Leknes, L., Riis F. and Fjeldskaar, W., 2009. *Abstract and oral presentation.*
Effects of erosion on reservoir fluid pressure and fault reactivation in the Barents Sea. EGU, Vienna, Austria, 19-24 April 2009.

Brenner, S.L., Gudmundsson, A. and Loetveit, I. F. 2004. *Abstract and oral presentation.*
Effects of mechanical layering on the emplacement of hydrofractures. 'Symposium Tektonik-Strukturgeologie-Kristallingeologie 10', Aachen, Germany, 31 March-2 April 2004.

Loetveit, I. F. and Gudmundsson, A., 2004: *Abstract and poster.*
Mechanical interaction between dykes and normal faults in volcanic rift zones. EGU I, Nice, France, 25-30 April 2004.

Gudmundsson, A. and Loetveit, I. F., 2004. *Abstract and poster.*
Dyke emplacement, graben formation, and eruptions in composite volcanoes. EGU I, Nice, France, 25-30 April 2004.

Gudmundsson, A. and Fjeldskaar, I., 2003. *Abstract and invited lecture.*
Effects of mechanical layering on dike emplacement, faulting, and surface deformation in volcanic rift zones. AGU 2003 Fall Meeting, San Francisco, 8-12 December 2003.

Loetveit, I. F. and Gudmundsson, A., 2003. *Abstract and poster.*
Aperture variation and fault-dyke interaction during dyke propagation in a layered rift zone. EGS-AGU-EUG Joint Assembly, Nice, France, 6-11 April 2003.

Fjeldskaar, I. and Gudmundsson, A., 2002. *Abstract and oral presentation.*
Propagation pathways and fluid transport in jointed and layered rocks. European Geophysical Society, 27th General Assembly, Nice, France, 22-26 April 2002.

Acknowledgements

First, I would like to thank my supervisor, Agust Gudmundsson, for excellent guidance along the way towards the submission of this thesis. He is a great source of knowledge, and his enthusiatic and inspiring way of teaching have been of great value to me.

The last part of this study was carried out at IRIS, supported by grants from the Research Council of Norway and StatoilHydro, as a part of the project 'Ice ages: subsidence, uplift and tilting of traps - the influence on petroleum systems' (Petromaks project 169291; 'Glacipet'). I want to express my gratitude to the Research Council of Norway and StatoilHydro for the support, and to IRIS for the opportunity to finish up this thesis.

My thanks also go to former fellow students of Agust, my former colleagues at Schlumberger Stavanger Research and my colleagues at IRIS for friendship and support during each stage of the project.

Finally, I want to express my gratitude to family and friends for their patience and support, especially my husband Arve, who has been a crucial support to me, and my children Grethe and Sigurd, the sunshine(s) of my life.

Ingrid Fjeldskaar Løtveit
Sola, April 2009.

Contents

Part I

Introduction and summary

Chapter 1

General introduction

The generation and maintenance of fracture-generated permeability depends on two basic mechanisms; the formation of extension fractures and the formation of shear fractures. Shear and extension fractures can be distinguished on the basis of the relative displacement across the fracture plane. In a shear fracture the displacement is parallel to the fracture plane, whereas in an extension fracture the displacement is perpendicular to the fracture plane.

Shear fractures, or faults, commonly develop from smaller fractures, such as sets of joints and extension fractures (Gudmundsson, 1992; Cartwright et al., 1995; Acocella et al., 2000), and can be major conduits for crustal fluids (Bruhn et al., 1994; Caine et al., 1996; Evans et al., 1997; Haneberg et al., 1999; Faybishenko et al., 2000). Their influence on the permeability is controlled by the present stress field. A change in the stress field may initiate and reactivate faults, and thus increase the temporary average permeability of a site by several orders of magnitude (Lee and Farmer, 1993; Gudmundsson, 2000b). In contrast, inactive faults may have very low permeability (Braathen et al., 1999) and thus work as barriers for the fluid flow in an area.

There are two types of extension fractures: tension fractures and hydrofractures. Tension fractures form when the minimum principal compressive stress is negative and are thus mostly limited to shallow depths in areas undergoing active extension, such as rift zones (Gudmundsson, 1992). Hydrofractures, however, can form at any depth, and are thus of greater importance when it comes to permeability than tension fractures. Hydrofractures are fractures generated by internal fluid overpressure, that is, they are driven open by any kind of crustal fluid, such as magma (dykes, sills and inclined sheets), geothermal water (mineral veins), oil, gas, and groundwater (many joints). Results from analytical modelling show that for a homogeneous host rock, the fluid overpressure in a hydrofracture generates very high crack-tip tensile stresses that often exceed the tensile strength of the host rock. It follows that hydrofractures are very important contributors to frac-

ture network development, and hence to increase in the overall permeability. In layered rocks, however, hydrofractures tend to be arrested, especially at contacts between layers of contrasting mechanical properties. The conditions that favor hydrofracture propagation, or arrest, are of vital importance for understanding the development of fracture systems.

External horizontal crustal stresses are important contributors to fracture development. Analytical models of unloading of the surface due to rapid erosion and deglaciation, conditions likely to have been operative in Norway and adjacent areas during the Pliocene-Pleistocene, results in a surface-parallel compressive stress that exceeds the vertical overburden stress. This compressive stress is known to favour the development of exfoliation fractures parallel to maximum principal stress, that is, parallel to the surface. Exfoliation fractures decrease rapidly in frequency with depth, but will, if they become interconnected, contribute significantly to bedrock permeability at shallow depths. In this thesis, the possible propagation pathways of a hydrofracture are discussed, considering propagation through homogeneous (Paper A-D) and layered (Paper A, B, D and E) host rocks with vertical and horizontal discontinuities (Paper A-C), as well as faults (Paper D).

The high compressive horizontal stresses associated with rapid glacial erosion may also lead to the generation and reactivation of reverse faults, and contribute to the linking up of fractures by faults. In the Norwegian part of the Barents Sea has been regarded as a province of major petroleum potential. The general findings are mainly gas reserves, the oil discoveries are mainly residual oil and therefore not of commercial interest. It is believed that the Pliocene-Pleistocene erosion, estimated at approximately 1-2 km (Berglund et al., 1986; Bjørlykke et al., 1989; Wood et al., 1989; Vorren et al., 1991; Linjordet and Grung-Olsen, 1992; Nyland et al., 1992; Riis and Fjeldskaar, 1992; Vågnes et al., 1992; Richardsen et al., 1993; Rasmussen and Fjeldskaar, 1996; Cavanagh et al., 2006), has affected the accumulation of hydrocarbons in the Barents Sea reservoirs (Nyland et al., 1992). The stress effect of erosion on fluid reservoirs, with application to the Barents Sea, is discussed in Paper F of this thesis.

The conditions for fracture development in relation to crustal fluid pressure and transport have implications for many fields, such as petroleum (Paper F) and geothermal (Paper A) exploration, volcanic risk assessment (Paper D) and groundwater transport (Paper B and C). Because of this wide spectrum of implications, a relatively detailed introduction follows in the first part of this thesis. The section below provides the basic motivation and the corresponding objectives for the research. Geologic and mechanical concepts related to propagation and fluid flow in rock fractures are reviewed in Chapter 2-4, followed by a brief description of the numerical methods used in Chapter 5. A summary of the main results and some main conclusions are given in Chapter 6 and 7 of the first part of this thesis. Part

II presents the scientific papers resulting from this study.

1.1 Motivation and objectives

The principal aim of this thesis is to contribute to improved understanding of the effects of stresses on permeability, interconnection of fractures, and fluid flow in fractured rocks, with application to fluid-filled reservoirs.

The results are important for many applied and academic fields, including:

- Petroleum exploration and production
- CO_2 storage
- Groundwater supply
- Geothermal exploration
- Volcanic risk
- Nuclear waste disposal

Chapter 2

Rock fractures

The term 'rock fracture' refers to any significant mechanical break in the rock that is primarily of tectonic origin. Fractures are the most common structures in the brittle part of the lithosphere. The term 'crack' is commonly used in models of rock; for example as regards the displacement of the fracture surface. Based on the deformation mechanism, there are three modes of cracks (Fig. 2.1). Mode I is the opening or tensile mode, where the crack surfaces move directly apart, producing tensile or extension fractures that develop perpendicular to the direction of minimum stress. Mode II represents the sliding or in-plane shear mode. The crack surfaces slide past one another in a direction perpendicular to the leading edge of the crack. Mode III is the tearing mode, where the crack surfaces move relative to one another and parallel to the leading edge of the crack. Mode II and Mode III represent shear fractures (Atkinson, 1987; Engelder, 1993; Hudson and Harrison, 1997; Broberg, 1999).

2.1 Extension fractures

2.1.1 Tension fractures

One of the two main types of extension fractures is the tension fracture. A tension fracture is generated when there is an absolute tension in the crust, that is, when the minimum compressive stress is negative. Thus they are most common in areas undergoing active extension, such as in rift zones and grabens at divergent plate boundaries. A tension fracture can only form close to or at the surface; below a certain crustal depth, a tension fracture must change into a shear fracture, that is, a normal fault. Based on the Griffith failure criterion the maximum depth, d_{max}, to which a tension fracture can propagate before it changes into a normal fault is (Gudmundsson, 1992, 1999):

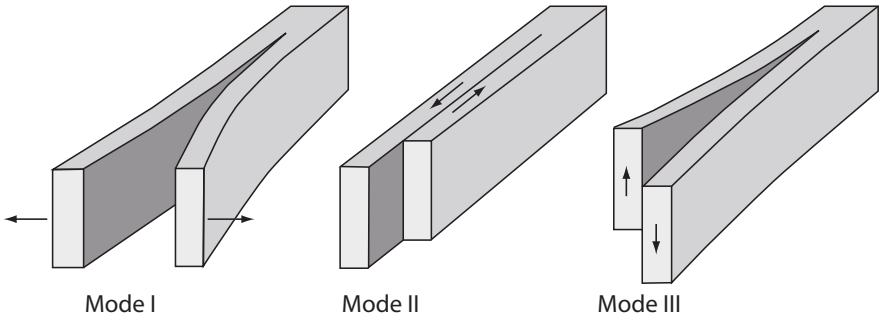

Figure 2.1: *The three basic modes of cracks used based on the displacement mechanism. Mode I is the opening or tensile mode, Mode II is the sliding or in-plane shear mode, and Mode III represents the tearing mode (modified from Twiss and Moores, 1992).*

$$d_{max} = \frac{3T_0}{\rho_r g} \tag{2.1}$$

where T_0 is the tensile strength of the rock, ρ_r is the rock density and g is the acceleration due to gravity.

The resulting normal fault may have a large opening at the surface, due to the fact that its near-surface part may be subject to absolute tension. They may transport large volumes of fluids, so they may be very important for the permeability in areas of absolute tension. Equation 2.1 is applied to tension fractures in typical Norwegian bedrock in Paper B, and to a tension fracture in a basaltic host rock in Paper C.

2.1.2 Hydrofractures

Hydrofractures are fractures partly or entirely generated by internal fluid pressure from crustal fluids such as gas, oil, magma, geothermal water or groundwater. They include dykes, sills, inclined sheets, mineral veins and many joints, as well as hydraulic fractures, which are fractures made with the purpose of increasing reservoir permeability. In some hydrofractures, the fluid that formed the fracture disappeared after formation. This is the case for many hydrofractures formed by the fluid pressure from gas, oil and groundwater, and is presumably the process behind the generation of many joints (Secor, 1965). In dykes, sills, inclined sheets and mineral veins, however, the fracture-generating fluid solidified in the fracture once it was formed.

Most hydrofractures are Mode I cracks, that is, extension fractures (Gudmundsson et al., 2001) that propagate in a direction parallel to the maximum compressive principal stress and perpendicular to the direction of minimum compressive stress. They are normally initiated when the internal fluid excess pressure (in excess of the minimum principal compressive stress) exceeds the tensile stress of the rock.

The fluid pressure that drives a hydrofracture open is the internal fluid overpressure, P_0, defined as:

$$P_0 = P_t - \sigma_n \tag{2.2}$$

Here, P_{t} is the total fluid pressure and σ_n is the normal stress on the hydrofracture. Since most hydrofractures are extension fractures the normal stress is equal to the minimum compressive principal stress, σ_3. 'Overpressure' is a well established term (Heimpel and Olson, 1994; Bonafede and Rivalta, 1999a,b). However, it is also referred to as driving pressure or driving stress (Pollard and Segall, 1987) or as net pressure. Fluid overpressure, as used here, should not be mixed up with abnormal pore formation pressure. In the latter case the the hydrostatic pressure usually is regarded as normal, and pressures below and above this state are referred to as subnormal and supernormal, respectively (Selley, 1998).

As long as the internal fluid overpressure exceeds the tensile strength of the host rock, hydrofractures will keep propagating and form their pathways by linking up discontinuities ahead of their tips. 'Discontinuities' refers to any mechanical breaks or fractures of low or zero tensile strength in the rock (Priest, 1993), and include contacts, joints, faults and other zones of weakness. The hydrofracture pathway is therefore largely determined by the stress field ahead of its tip. A discontinuity in a favourable orientation to the present stress field has commonly a tendency to maintain a certain discontinuity-parallel permeability (Gudmundsson et al., 2001).

2.2 Shear fractures

A fracture where the relative displacement is parallel to the fracture plane is called a shear fracture, or a fault if the displacement is large. Faults strongly influence the permeability of a host rock (Barton et al., 1995; Finkbeiner et al., 1997; Gudmundsson, 2000b; Gudmundsson et al., 2001) and are commonly major conduits of water (Bruhn et al., 1994; Caine et al., 1996; Evans et al., 1997; Haneberg et al., 1999; Faybishenko et al., 2000).

Faults may initiate at small-scale shear fractures, or more commonly develop during the linking up of small fractures of various types. They normally grow by

linking up of gradually larger segments. These segments may be offset joints, as discussed in Papers B and C.

Hydrogeologically, large fault zones are made up of two units; the fault core and the damage zone. The fault core mainly consists of breccia or gouge. The damage zone normally consists of numerous fractures of various sizes (Bruhn et al., 1994; Caine et al., 1996; Evans et al., 1997; Seront et al., 1998), where the fluid transport occurs through the network of the fractures that are interconnected (Caine et al., 1996; Sibson, 1996). The permeability of the fault core is normally significantly less than that of the damage zone, which generally is the main conduit for fluid flow in a fault zone. This may be due to occurrence of gouge, a very fine grained material that forms due to frictional sliding and pulverisation during fault slip, or slickensides, glass surfaces that form due to grain melting during fault slip, both of which reduce the permeability of the fault core, in particular the permeability perpendicular to the fault plane. Slickensides may, however, also increase the permeability parallel to the slip surface as a result of mismatch of the smooth walls.

Fault slip most commonly occurs at the contact between the damage zone and the fault gouge or breccia of the fault core. This is partly due to the minimum sliding friction between two layers of very different mechanical properties (Nelson, 1985) and partly due to stress concentrations that occurs at contacts where there is a sharp contrast in elastic properties. During slip the pores and small fractures that meet with the fault plane interconnect, so that the overall fault, particularly the fault core, suddenly experience a significant increase in permeability (Gudmundsson, 2000b).

The activity, and the permeability, of a fault zone are controlled by the current stress field, and the angle that the fault makes to the principal stress directions. The permeability of the damage zone may also be strongly affected by the stress field as the majority of the fractures are extension fractures oriented subparallel to the fault plane (Gudmundsson et al., 2001). Thus when the maximum principal compressive stress is at a high angle to the fault plane, many fractures in the damage zone tend to close and reduce the fluid transport. When, however, the maximum principal compressive stress makes a small angle with, or is parallel to, the fault plane, fractures in the damage zone tend to be open and increase the fluid transport.

Chapter 3

Fluid flow in fractures and faults

Permeability is a measure of how easily fluid flows through the rock. In porous media, the permeability is determined by the interconnection of pores. In solid rock, however, the porosity is normally quite low, due to diagenesis processes such as compaction and cementation, so that the fluid transport mainly takes place through interconnected fractures (Nelson, 1985; Singhal and Gupta, 1999). This chapter presents some physical principles related to fracture-generated permeability, including analytical models on the volumetric flow rate of the fluid flow in fractures, as well as analytical models on the crack tip stresses and aperture associated with overpressured fractures.

All transportation of fluid in rocks originates from a primary fluid source, and ends up as the fluid gets trapped underneath a low-permeable rock layer and accumulates in a reservoir, or as it reaches the surface. The source rock of hydrocarbons is most commonly organic rich sedimentary rock. The detailed mechanism of the transport of hydrocarbons from the source rock is poorly understood, but it is suggested that hydrofractures play an important role in migration hydrocarbon (e.g. Iliffe et al., 1999; Nunn and Meulbroek, 2002). Groundwater and geothermal water originate from the precipitation at the Earth's surface (Domenico and Schwartz, 1998), and the source rock is the aquifer that transports water from the catchment area to the reservoir. The primary source of magma is in the upper part of the mantle, where partial melting takes place (Gudmundsson, 2000c; Sigurdsson et al., 2000). The term 'fluid source' generally refers to a zone of fluid accumulation.

Consider a fluid source, any kind of fluid reservoir, subject to a fluid excess pressure p_e, defined as the pressure in excess of the minimum compressive (maximum tensile) principal stress, σ_3, in the roof of the reservoir. The roof of the reservoir will rupture and initiate a hydrofracture when:

$$p_l + p_e \geq \sigma_3 + T_0 \tag{3.1}$$

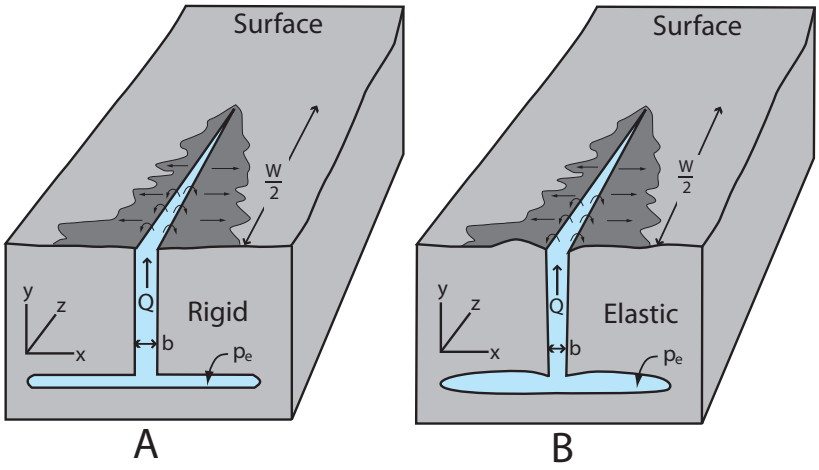

Figure 3.1: *Models of a vertical fluid-filled fracture supplied from a fluid source. The aperture, b, the width, W, the excess fluid pressure, p_e, and the volumetric flow rate, Q, are indicated. Model A refers to a rigid host rock, and B to an elastic host rock.*

where p_l is the lithostatic stress at the depth of the reservoir, and T_0 is the in situ tensile strength of the host rock at the roof of the reservoir.

Once a hydrofracture has been formed, and made its pathway by linking up of discontinuities in the host rock, the volumetric rate of flow can be estimated.

3.1 Fluid flow in a single fracture

Flow along a single fracture can be modelled by using a special solution of the Navier-Stokes equations for flow between parallel plates. In hydrogeology, it is commonly referred to as the cubic law (Bear, 1993), because the volumetric flow rate is assumed to be proportional to the cube of the fracture aperture.

During the propagation of a hydrofracture, the host rock can respond in two ways; as rigid or as elastic (Fig. 3.1). In a rigid host rock, the fracture is entirely selfsupporting and non-deforming. The assumption of a rigid host rock is commonly made when modelling groundwater flow in fracture systems in the uppermost part of the crust (Bear, 1993; Taylor et al., 1999). At deeper levels, however, the host rock is likely to deform in an elastic way in response to the changes in fluid pressure.

The volumetric flow rate through a selfsupporting vertical fracture (denoted by superscript s) in a rigid host rock, as shown in Figure 3.1 (Model A), is given

by (Gudmundsson, 2001):

$$Q_y^s = \frac{b^3 W}{12\mu}\left[(\rho_f g) - \frac{\delta p_e}{\delta y}\right] \tag{3.2}$$

where b is the fracture aperture, W the width of the fracture in a direction perpendicular to the flow direction, μ the dynamic (absolute) fluid viscosity, ρ_f the fluid density, g the acceleration due to gravity, and $\delta\rho_e/\delta y$ the gradient of the excess pressure in the direction of flow.

For an elastic host rock, where the fracture walls are free to deform during fluid transport, a buoyancy term must be added to Equation (3.2). This is because the weight of the rock above the reservoir must be supported by its internal fluid pressure, and because the different densities of the host rock, ρ_r and the fluid ρ_f. The volumetric rate of fluid flow in a vertical elastic fracture (denoted by superscript e) (Model B in Fig. 3.1) then becomes:

$$Q_y^e = \frac{b^3 W}{12\mu}\left[(\rho_r - \rho_f)g - \frac{\delta p_e}{\delta y}\right] \tag{3.3}$$

For non-vertical fractures, such as shear fractures and faults, with a certain dip angle α, Equation (3.2) and Equation (3.3) is modified by taken into account the component of gravity in the dip direction, $gsin\alpha$ (Gudmundsson, 2001). Equation (3.2), the volumetric flow rate of fluid flow in a non-vertical fracture in a rigid host rock, then becomes:

$$Q_L^s = \frac{b^3 W}{12\mu}\left[(\rho_f g \sin\alpha) - \frac{\delta p_e}{\delta L}\right] \tag{3.4}$$

where δL is the part of the dip dimension of the fracture along which the fluid flows at a volumetric rate Q_L. For non-vertical fractures in an elastic host rock, the volumetric flow rate of fluid flow is then:

$$Q_L^e = \frac{b^3 W}{12\mu}\left[(\rho_r - \rho_f)g\sin\alpha - \frac{\delta p_e}{\delta L}\right] \tag{3.5}$$

In Equations 3.2 - 3.5, the fluid flow in a single fracture is calculated. This is commonly a reasonable approximation for fluid flow in a cluster of interconnected fractures, as it may act both mechanically and hydraulically as a single fracture. For a fault zone, modelling fluid flow through a single fracture applies for the whole fault zone during slip, whereas during interseismic periods this only applies to the damage zone. The core may then be considered as a porous medium, so that the fluid flow through this part of the fault can be modelled using Darcy's law on fluid transport in porous media (Caine et al., 1996). However, the previous analytical solutions for fluid flow can easily be extended to equations for fracture

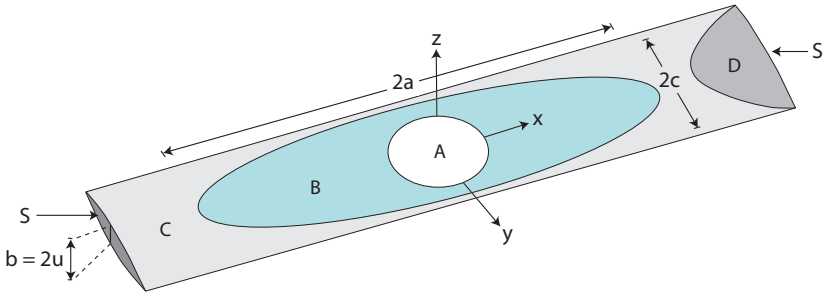

Figure 3.2: *In an elastic host rock, cracks are modelled having one of three basic shapes. A and B are interior cracks, C is a through crack and D is a part-through crack (Gudmundsson, 2000a).*

sets (Bear, 1993), which may apply to parallel set of fractures in near surface-conditions and away from large fault zones (Singhal and Gupta, 1999).

Equations 3.5 and 3.3 have been applied in Paper A of this thesis, for estimation of the dimension of a hydrofracture network, conceptualised as a single hydrofracture, based on measured volumetric flow rates of a typical hot spring in Iceland.

The aperture, b, in Equations 3.2 - 3.5 is assumed constant, whereas in an elastic host rock it would normally depend on the fluid pressure of the fracture and the state of stress in the host rock. The effect of fluid overpressure on the fracture aperture is discussed in the following section.

3.2 Crack stress and opening displacement

Based on how they appear in the solid layer that hosts them, cracks can be put into three main categories or types (Fig. 3.2). The first type includes cracks that are located in the interior of an elastic layer, and do not propagate to any of the surfaces of the layer. These are normally referred to as elliptical interior cracks or 'penny-shaped' cracks. In the second type, the cracks extend partly into the thickness of the hosting layer and are referred to as part-through or 'thumbnail' cracks. The third type is cracks that extend through the whole hosting layer. Cracks of this type are called 'through-the-thickness' cracks, through cracks or tunnel cracks.

For the growth of a fracture to be possible, the tensile stresses at its tip must exceed the tensile strength of the rock. To calculate crack-tip stresses and aperture

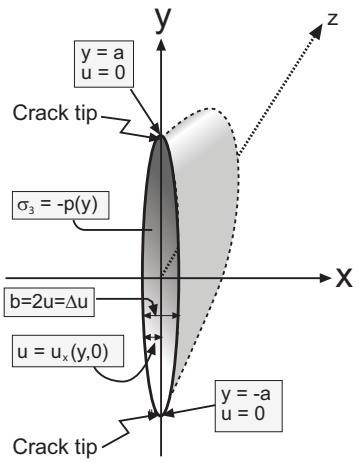

Figure 3.3: *A three-dimensional mathematical crack located along the vertical y-axis, where σ_3 is the stress inside the crack tips, Δu is the aperture of the crack, and $2a$ is the total length of the crack.*

associated with a fracture subject to a certain internal fluid pressure, the fracture can be modelled either as a flat elliptical hole, or as a mathematical crack of zero aperture. In both models the fluid-filled fracture is regarded as an interior crack in a homogeneous host rock. These models are the basic models for analysing hydraulic fracturing in the petroleum industry (Valko and Economides, 1995), and are also widely used in fracture models in general (Maugis, 2000; Jaeger et al., 2007).

3.2.1 Mathematical crack model

First consider fluid-filled fracture modelled as a two-dimensional mathematical crack located on the vertical y-axis and defined by $x = 0, -a \leq y \leq a$, as shown in Figure 3.3. The fracture is subject to an internal fluid pressure given by the even function $p(y) = p(-y)$, so that the pressure is the same on the fracture walls on either side of the x-axis.

The general solution procedure for the tip stresses and the opening displacements of elastic cracks has been summarised by Sneddon and Lowengrub (1969), Valko and Economides (1995) and Maugis (2000). Most authors provide the specific solutions for a constant fluid overpressure, but few have considered solutions of a linear pressure gradient. In this thesis, both types are considered, though the focus is on the stresses and displacements associated with linear overpressure

gradients, as these may be expected in many propagating natural hydrofractures.

The general solution for normal displacement of the crack walls $u = u_x(y, 0)$ in the x-direction is:

$$u = \frac{4(1-\nu^2)}{\pi E} \int_y^a \frac{tq(t)dt}{(t^2-y^2)^{1/2}} \tag{3.6}$$

where:

$$q(t) = \frac{p(y)dy}{(t^2-y^2)^{1/2}}, \qquad \textit{for} \quad 0 < t < a \tag{3.7}$$

E is Young's modulus, describing the stiffness of the host rock, ν is Poisson's ratio and y is the coordinate along which the fracture is located.

Since most natural hydrofractures are pure extension fractures (Gudmundsson et al., 2001), the normal stress on the hydrofracture is the minimum principal compressive stress, σ_3. Inside the crack $\sigma_3 = -p(y)$, for $0 \leq y \leq a$, and outside the crack tips, for $y > a$, the stress $\sigma_3(y, 0)$ is:

$$\sigma_3 = -\frac{2y}{\pi} \int_0^a \frac{tq(t)dt}{(y^2-t^2)^{1/2}} \tag{3.8}$$

Consider the case of a constant overpressure where $p(y) = P_0$, as is used for the boundary-element models in Paper D. By substituting this in Equation (3.7), we get $q(t) = P_0\pi/2$. The normal displacement of the crack walls for a hydrofracture subject to constant fluid overpressure then becomes:

$$u = \frac{2(1-\nu^2)P_0}{E}(a^2-y^2)^{1/2} \tag{3.9}$$

The opening or the aperture of the fracture, $b = \Delta u$, is twice the normal displacement, so that $\Delta u = 2u$. The result of Equation (3.9) implies that a fracture in a homogeneous, isotropic rock is elliptical in shape (Sneddon and Lowengrub, 1969; Gudmundsson, 2000b). The maximum tensile principal stress outside the crack tips can be obtained from Equation (3.8) by substituting $q(t) = P_0\pi/2$ from Equation (3.7):

$$\sigma_3 = -P_0 y \left[\frac{1}{(a^2-y^2)^{1/2}} - \frac{1}{x} \right] \tag{3.10}$$

If $y \rightarrow a$, when the tip of the hydrofracture is approached from outside the tip, then $\sigma_3 \rightarrow -\infty$, that is, the tensile stress becomes infinite.

A linear variation in fluid pressure, which is assumed common in hydrofractures, is used in the boundary-element models in Papers (A, B and C). There are at least three factors that lead to a variation in the internal fluid pressure. First, there is a difference in density between the fluid and the host rock. The host rock

commonly behaves elastically and a buoyancy term has to be added to the overpressure. Secondly, there are changes in the stress acting normal to the fracture. This stress depends on Young's modulus and Poisson's ratio, and it follows that in a layered crust the stress can vary considerably. Thirdly, the overpressure depends on the dip of the hydrofracture. Normally, the hydrofracture is propagating in a direction that is normal to σ_3, but it is also common that a hydrofracture follows weaknesses in the rock that are oblique to σ_3 so that the normal stress becomes higher and the fluid overpressure lower.

Consider a line crack where the fluid overpressure $p(y)$ varies from a maximum value P_0 at the centre of the crack by a linear gradient $p_1 y$ towards the tips:

$$p(y) = P_0 + p_1 y \tag{3.11}$$

By using this equation, the aperture $b = \Delta u = 2u$ can be obtained from Equations (3.6) and (3.7) as:

$$\Delta u = \frac{4(1-\nu^2)}{E}\left[P_0 m + \frac{p_1}{\pi}\left(am + y^2 ln\frac{a+m}{y}\right)\right] \tag{3.12}$$

where:

$$m = (a^2 - y^2)^{1/2} \tag{3.13}$$

and a is half the fracture length. Equation (3.12), which represents the aperture variation for a fracture subject to linearly varying fluid overpressure, is far more complex than Equation (3.9) for constant overpressure. By plotting the aperture as a function of y, the result shows a smooth curve variation not unlike an ellipse. Both a constant overpressure and linearly varying overpressure for a hydrofracture in a homogeneous, isotropic rock yield smoothly varying and similar opening displacement profiles. Maximum principal tensile stress outside the crack tips is derived from the Equations 3.7 and 3.8:

$$\sigma_3 = -\frac{2p_1}{\pi}\left[\frac{ya}{(y^2 - a^2)^{1/2}} - y \arcsin\frac{a}{y}\right] \tag{3.14}$$

This illustrates that when $y \to a$, the hydrofracture being approached from outside the tip, the maximum tensile principal stress becomes infinite, $\sigma_3 \to -\infty$. For the mathematical models used here the tensile stresses will approach infinity or be very high, whether the fluid overpressure is constant or varying linearly.

In Paper E the opening displacement profiles resulting from a constant, linear as well as a polynomial varying fluid overpressure are presented. The results indicate that all three types of overpressure variations within a hydrofracture yield similar aperture shapes, but different aperture sizes.

3.2.2 Elliptical hole model

The hydrofracture can also be modelled as an elliptical hole. The major axis is $2a$ and the minor axis $2u$, so that $2u$ is the aperture. When the hydrofracture is subject to a constant fluid overpressure P_0, the minimum principal stress σ_3 at the tips is:

$$\sigma_3 = -P_0[\frac{2a}{u} - 1] \tag{3.15}$$

If the crack tips are exposed and measurable in the field, the crack-tip tensile stress can be calculated from the radius of curvature of the tip. If the radius of curvature is $r_c = u^2/a$, the formula is given by:

$$\sigma_3 = -P_0[2(a/r_c)^{1/2} - 1] \tag{3.16}$$

The crack stress calculations, whether they are based on the mathematical crack model or the elliptical hole model, show that for a homogeneous host rock the crack tip tensile stresses are very high, or reaches infinity. Infinite stress is, however, never reached in the host rock, as plastic deformation and microcrack opening at the hydrofracture tip will relief part of the stress.

In the models for fluid flow, aperture and crack stress, the fractures are idealised, as having smooth shapes. By contrast, all natural fractures have irregular opening profiles. Variations in fracture aperture are important factors for the fluid transport in fractured reservoirs, this follows because the fluid flow tends to concentrate on those parts of a fracture where the aperture is largest, often referred to as flow channelling (Tsang and Neretnieks, 1998).

In nature, both extension fractures and shear fractures may be filled with secondary minerals, such as quartz, zeolite or calcite, which affect their ability to transport fluids. Fractures completely filled with minerals are normally impermeable and thus barriers to flow, whereas partly mineral-filled fractures (Fig. 3.4), may contribute positively to the permeability. This is partly due to channels within the mineralised fracture, and partly because the mineral infills increase the stiffness of the fracture and thus its resistance to closure during normal compression. In carbonate rocks, the fracture geometry of extension and shear fractures may also be affected by dissolution, resulting in vuggy fractures (Aguilera, 1995). Due to dissolution, normally by acid fluids, of the fracture walls, the shapes of vuggy fractures are circular or elliptical in plan view (Fig. 3.5). In three dimensions they normally have geometry of a sphere or an ellipsoid, which makes them highly resistant to normal compression and subsequent closure. This means that their appearance highly increase the permeability of carbonate rocks. Thus, the subject of dissolution is of crucial importance when dealing with permeability in carbonate reservoirs.

Fracture apertures, and fracture propagation, also depend greatly on the mechanical properties, as well as local and regional stress fields operating on the host rock. These important factors are discussed in the following chapter.

Figure 3.4: *Partly mineralised and crystallised fracture. View northwest.*

Figure 3.5: *An original extension fracture cutting through a succession of limestone and shale has resulted in vuggy fractures after being subject to dissolution at Lavernock Point, South Wales. The limestone layers are the ones most affected by dissolution. The length or dip dimension of the extension fracture is approximately 50 cm.*

Chapter 4

Stress effects on fracture propagation

4.1 Local stress effects

Based on the analytical expressions on crack tip stresses provided in the previous chapter (Eqs 3.8, 3.10, 3.14, 3.15 and 3.16), it is expected that all fractures subject to internal fluid overpressure will continue their propagation all the way to the surface. Field studies, however, indicate that most hydrofractures never reach the surface, but rather become arrested at various depths in the crust (e.g. Baer, 1991; Gudmundsson, 1999; Marinoni and Gudmundsson, 2000; Gillespie et al., 2001; Gudmundsson et al., 2001). The propagation of fluid-filled fractures is dependent on the homogeneity of the host rock, and thus the absence of conditions favourable for arrest, that is, abrupt changes in mechanical properties, horizontal discontinuities, and stress barriers.

One of the most important mechanical properties that affect the propagation of a fluid-filled fracture is the stiffness of the host rock, that is, the Young's modulus, E (cf. Chapter 5.1). Layers with high Young's modulus are often referred to as stiff, whereas layers with low Young's modulus are referred to as compliant or soft.

The conditions favourable for arrest are very common in mechanically layered rock masses, where hydrofractures commonly become arrested at contacts between stiff and soft layers. The stiff layers tend to magnify the crack tip tensile stresses associated with the propagating hydrofracture, whereas soft layers tend to suppress the tensile stresses (Gudmundsson et al., 2001). Thus, the soft layers tend to favour hydrofracture arrest. Experiments on man-made hydraulic fractures confirm that soft layers are commonly more effective in stopping fractures than stiff layers (Charlez, 1997; Yew, 1997).

Figure 4.1: *Hydrofractures propagating through a mechanically layered sedimentary rock of alternating stiff limestone and soft shale layers, near to Llantwit Major, South Wales. Due to the low or zero tensile strength of the soft shale layer, the hydrofractures must follow shear fractures to continue their propagation as they enter the shale.*

In addition, contrasting mechanical properties greatly affect the aperture of a hydrofracture. In soft layers, the aperture is normally larger than in stiff layers. This follows because soft layers are likely to deform rather than sustain stress, due to low tensile strength. The resulting aperture variation in mechanically layered rocks lead to flow channelling (Tsang and Neretnieks, 1998), and may be described analytically by an irregular fluid overpressure variation based on Fourier series (Kusumoto and Gudmundsson, 2009).

Very soft layers commonly have very low, or no, tensile strength, and may to some extent behave ductile. However, they normally have shear strength, and may thus respond to stresses, such as those associated with a propagating hydrofracture, by shear failure. A propagating hydrofracture is therefore likely to change its vertical direction and follow an inclined shear fracture, when entering a significantly soft rock layer (Fig. 4.1).

Horizontal discontinuities, such as weak contacts (referring to contacts with low or no tensile strength), often occur in layered rocks. The opening up of weak contacts, such as due to an approaching hydrofracture, is mainly due to downward deflection of the lower wall, whereas the upper wall remains straight, a geometry related to the Cook Gordon mechanism for stopping cracks (Cook and Gordon,

Figure 4.2: *A hydrofracture has joined with a weak horizontal contact resulting in a T-shaped fracture. The steel tape has a length of 50 cm.*

1964; Atkins and Mai, 1985). If a hydrofracture link up with such a contact, it may open up to form a T-shaped fracture (Valko and Economides, 1995), as shown in Figure 4.2 .

Stress barriers are rock bodies with local stress fields that are unfavourable to the propagation of the considered type of fractures, whether they are shear fractures or extension fractures (Gudmundsson, 2002). They are particularly common in mechanically layered rocks, where they determine whether hydrofractures become restricted to single layers or not, and thus whether a vertically interconnected fracture network develops. Hydrofractures are generally vertical, so that the stress field working normal to the fracture walls are considered stress barriers. When subject to horizontal extension, the stiff layers in the rock mass are likely to favour the initiation and propagation of hydrofractures, whereas the soft layers are likely to suppress the stress and favour arrest (Gudmundsson and Brenner, 2001).

For a layered rock mass subject to a horizontal compressive stresses, the stiff layers tend take up most of the compressive stress, becomes highly stressed, and are thus likely to suppress the crack tip tensile stress of a propagating hydrofracture (Gudmundsson, 1990; Gudmundsson and Brenner, 2001). The stiff layers may then act as stress barriers and cause hydrofracture arrest. The mechanisms for arrest and deflection of hydrofractures are discussed in Paper E of this thesis.

There are also mechanisms that may change the stress condition so as to

become favourable for hydrofracture propagation. Gudmundsson and Brenner (2001) have suggested that a homogenisation of the stress field favour further propagation of hydrofractures.

For faults and shear fractures, stress fields unfavourable for slip are normally the ones with low angle to the fault plane. Large fault zones, however, are likely to experience a local rotation of the stress field within the damage zone. This follows because the observed increase in fracture frequency with decreasing distance to the fault core (Gudmundsson, 2004; Faulkner et al., 2006) lead to a gradual change in the elastic properties of the damage zone (Heap and Faulkner, 2008). This gradual change in elastic properties results in a gradual rotation of the stress field, so that the local stress field close to the fault core may become more favourable for fault slip than the regional stress field (Faulkner et al., 2006).

4.2 Regional stress regimes

The current stress field largely controls fluid flow in, and therefore the permeability of, fractured reservoirs (Faybishenko et al., 2000; Gudmundsson, 2000a). This follows because fractures are sensitive to changes in the stress field and deform much more easily than circular pores, and because the stress field contributes to the fluid overpressure (cf. Eq. 2.2 in Chapter 2.1.2).

Information on the present day stress field can be obtained by various different stress indicators sampled in different depth intervals. The most widely used indicators are earthquake focal mechanisms, well bore breakouts and drilling-induced fractures, in-situ stress measurements and young geologic data, all of which are collected and added to the World Stress Map project database (www.world-stress-map.org).

Determining an earthquake focal mechanism solution includes the use of P-wave first-motion polarities. When these are recorded at a number of seismograph stations in a stereographic plot, the two nodal planes can be defined; one of them is the fault plane and the other an auxiliary plane with no geological significance (Shearer, 1999). A preferred orientation of earthquake faults can be can give information on the orientation of the regional stress field in the seismogenic part of the crust.

Well-bore breakouts develop in a direction parallel to the minimum horizontal stress axis, σ_h, if the tangential stress at the borehole wall overcomes the compressive (or shear) strength of the rock. From this, information on the orientation of the maximum horizontal stress, σ_H, can be inferred (Zoback et al., 1985; Amadei and Stephansson, 1997; Zoback, 2007). Normally, borehole breakouts can give information on the in situ stress field at depths of 1-4 km, in some cases to greater depths (Zoback et al., 1989). Drilling induced fractures occur at an angle of 90^o

to the well bore breakouts, and thus infer the orientation of maximum horizontal stress, S_H (e.g. Brudy and Kjørholt, 2001).

Hydraulic fracturing is a technique frequently used by the petroleum industry to increase reservoir permeability and to determine the in-situ stress field. During the experiment, a depth interval of the wellbore is isolated by packers and pressurised by injected fracturing fluids until an extension fracture develops in the direction of maximum horizontal stress, σ_H. The shut-in pressure, that is, the pressure required for keeping a fracture open, is assumed equal to the minimum principal horizontal stress, σ_h, whereas the maximum horizontal principal stress, σ_H, is found from the breakdown pressure, which is the fluid pressure at which the fracture developed (Kim and Franklin, 1987).

Paleo-stress fields can be determined from hydrofractures and fault slip data (slickensides) to support analyses of geological structures. Hydrofractures are mostly pure extension fractures, that is, they generally form in a direction that is perpendicular to the minimal principal stress and thus parallel to the other two principal stresses. Slickenside lineations provide the direction and sense of motion on individual fault planes (Angelier, 1984; McClay, 1987).

Earthquake focal mechanisms together with in-situ measurements are the most important sources of information on trends and magnitudes of the principal stresses. The in-situ stress field in an area is composed of plate-wide continental stresses influenced by regional and local effects. In this thesis, the theoretical and general study on fracture-generated permeability has been applied to Iceland and Norway.

4.2.1 Stress regimes in Iceland

Iceland is situated on the Mid Atlantic Ridge, at the divergent plate boundary between the North America plate and the Eurasian plate. Thus the regional stress regime in Iceland is clearly extensional, resulting in active rift zones and transform zones associated with massive volcanism and seismicity. Angelier et al. (2004) reconstructed the regional stress regimes in Iceland based on stress inversions of earthquake focal mechanisms from 126,588 earthquakes, recorded from July 1991 to July 1999 (Fig. 4.3).

4.2.2 Stress regimes in Norway

The in-situ stress field in Norway (Fig. 4.4) is affected by several regional stress generating mechanisms, that is ridge push, post-glacial uplift, and erosional unloading and loading (Bungum et al., 1991; Byrkjeland et al., 2000; Fjeldskaar et al., 2000; Hicks et al., 2000).

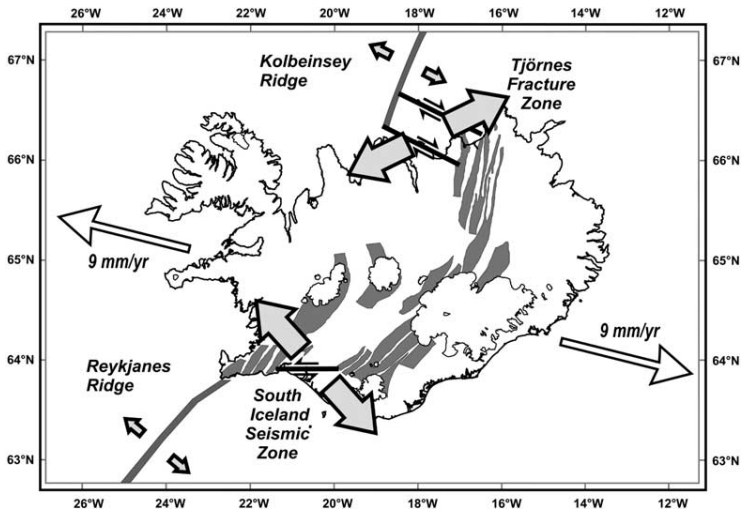

Figure 4.3: *Overview of the regional stress regimes in Iceland based on stress inversion of earthquake focal mechanisms. From Angelier et al. (2004).*

The ridge push is a combination of gravitational force and horizontal compressive stress generated by dyke injections originating from the Mid-Atlantic spreading ridge, and by definition it should be perpendicular to the spreading ridge. Thus, the NW-SE/ WNW-ESE trending horizontal compressive stress, and the observed tendency for reverse to strike-slip faulting, in offshore areas of Norway is assumed related to ridge push, whereas the tendency to normal to strike-slip in onshore areas must be explained by other mechanisms (Bungum et al., 1991; Byrkjeland et al., 2000; Hicks et al., 2000).

The present post-glacial uplift of Fennoscandia is estimated to a maximum value of 850 m (Mörner, 1980; Rohr-Torp, 1994), and is thus likely to have a major effect on the regional stress field. The contours of the present rates of uplift of Fennoscandia show a dome of an elliptical shape (Mörner, 1980; Fjeldskaar, 1997; Gudmundsson, 1999; Fjeldskaar et al., 2000). The result of modelling the post-glacial uplift by using bending of a circular, elastic crustal plate shows that the doming-generated stresses changes from being tensile in the central part to being compressive in marginal parts, and in all parts of the plate the stresses are large enough to initiate, or reactivate, fracture systems (Gudmundsson, 1999). Thus, the post-glacial uplift may be an important factor in increasing the hydraulic conductivity. It has been demonstrated that there is a linear relationship between the water yield in wells and the present rate of the post-glacial doming (Rohr-Torp, 1994; Morland, 1997).

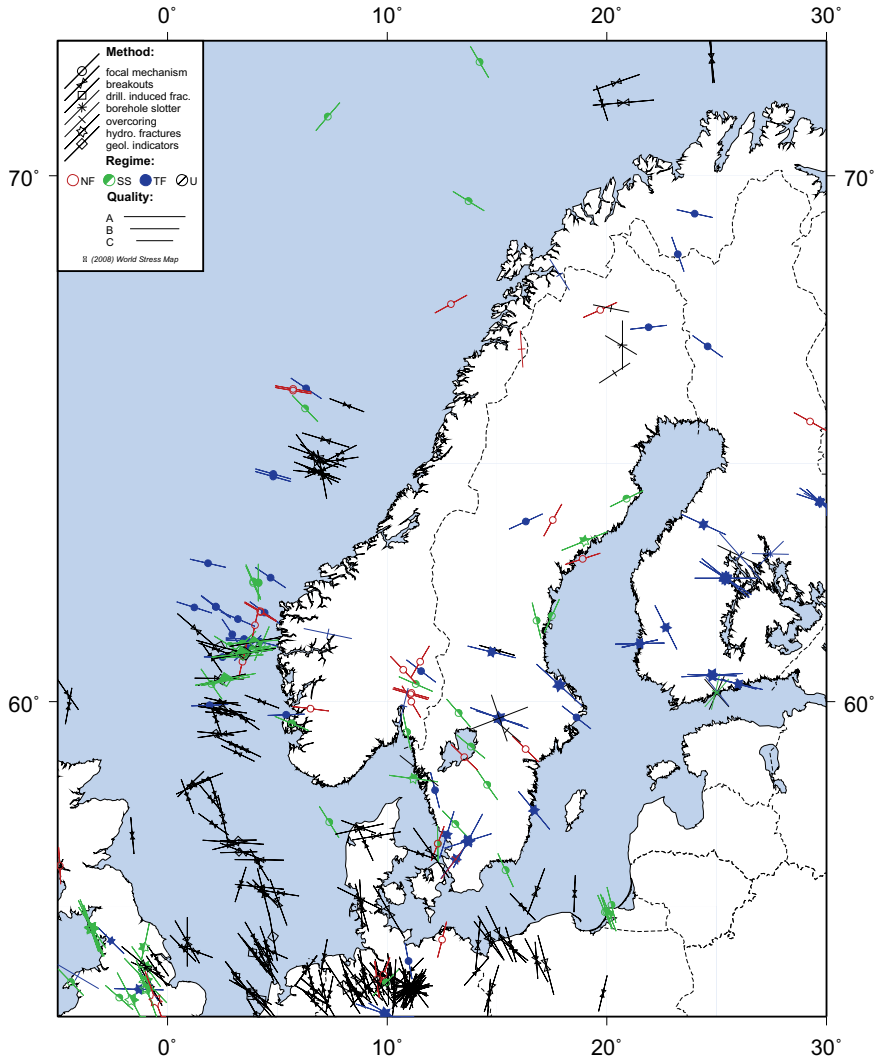

Figure 4.4: *Map showing the present stress fields in Scandinavia. The measurement methods, their quality and the stress regimes are indicated. Red refers to normal faulting (NF), green indicates strike-slip (SS), blue indicates thrust faulting (TF) and U refers to an unknown tectonic regime. From Heidbach et al. (2008).*

The stress field in the Norwegian part of the Barents Sea is generally difficult to establish. There are no earthquake focal mechanism solutions available, due to low levels of seismic activity and large distances to any seismic stations, so that the stress measurements in this area are solely based on borehole breakouts (Hicks et al., 2000). The in-situ stress generally show a N-S direction (Hicks et al., 2000), as well as a E-W direction in the west (note that in Figure 4.4 only the high quality measurements are considered, which means that several of the N-S oriented measurements Hicks et al. (2000) are referring to are excluded). The area has been subject to massive glacial erosion during the last 3 Ma. The glacial erosion in the norwegian part of the Barents Sea has been estimated by several authors (Berglund et al., 1986; Bjørlykke et al., 1989; Wood et al., 1989; Vorren et al., 1991; Linjordet and Grung-Olsen, 1992; Nyland et al., 1992; Riis and Fjeldskaar, 1992; Vågnes et al., 1992; Richardsen et al., 1993; Rasmussen and Fjeldskaar, 1996; Cavanagh et al., 2006) and is assumed to be in the range of 1000-2000m, increasing north. The stress field in the Barents Sea is very likely to be affected by this amount of erosion.

4.2.3 Stress effects of erosion

The effects of erosion can be modelled as stress changes resulting from the removal of sediments of a given thickness as shown in Figure 4.5. Before erosion, the maximum principal stress is equal to the vertical stress, so that $\sigma_1 = \sigma_v$, and both vary as the overburden pressure, thus (Jaeger and Cook, 1979):

$$\sigma_v = \sigma_1 = \rho_r g h \tag{4.1}$$

where ρ_r is the rock density, h the rock thickness, and g is the acceleration due to gravity. The assumption that the vertical stress is due to overburden pressure is commonly made and generally supported by stress data worldwide (Zoback, 1992; Amadei and Stephansson, 1997; Zoback, 2007).

An initial state of lithostatic stress assumed, which is reasonable for an old crust that has not been subject to major tectonic stresses for a long time (e.g., Jaeger and Cook, 1979; Amadei and Stephansson, 1997). Lithostatic state of stress is defined as isotropic stress, so that all the principal stresses are equal ($\sigma_1 = \sigma_2 = \sigma_3$), where the stress increases proportionally with depth in the crust. Furthermore, the rate of increase of stress is determined by the density of the crustal rocks, in accordance with Equation (4.1).

For a confined rock body, that is, one that cannot expand laterally, and in the absence of tectonic strain and stress, the intermediate and minimum compressive principal stresses, σ_2 and σ_3, may be estimated crudely from the following formula

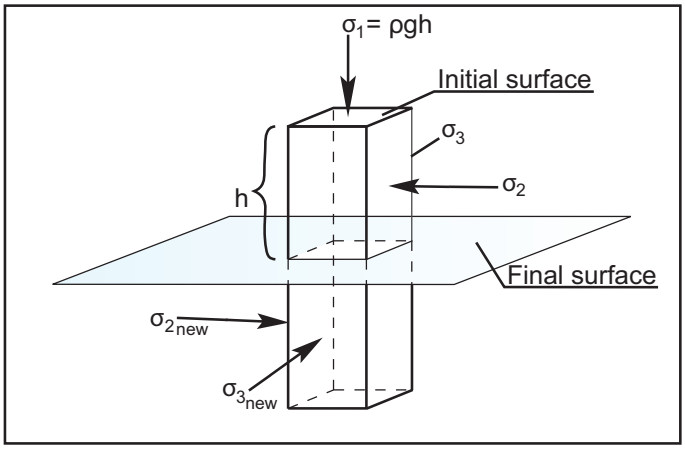

Figure 4.5: *During unloading from an initial surface to a new surface (marked as final surface), all the principal stresses change. Modified from Turcotte and Schubert (2002).*

(cf. Jaeger and Cook, 1979; Turcotte and Schubert, 2002):

$$\sigma_2 = \sigma_3 = \frac{\nu}{(1-\nu)}\sigma_1 = \frac{\nu}{(1-\nu)}\rho_r g h \tag{4.2}$$

After a sudden erosion to a depth h in the crust, it follows from Equation (4.1) that since h = 0, the vertical principal stress, σ_1, at that depth becomes zero (assuming any fluid pressure on the surface to be negligible). Thus, from Equation (4.1), the change in vertical stress is $\Delta\sigma_1 = -\rho_r g h$. Before the glacial erosion, the state of stress at crustal depth h was assumed lithostatic, so that the horizontal principal stresses at that time were equal to the vertical stress, or $\sigma_1 = \sigma_2 = \sigma_3$. After the erosion the horizontal principal stresses at depth h become reduced; not to zero, however, but rather to a value given by Equation (4.2). Thus, their changes, $\Delta\sigma_2$ and $\Delta\sigma_3$, due to the erosion are:

$$\Delta\sigma_2 = \Delta\sigma_3 = \frac{\nu}{(1-\nu)}\Delta\sigma_1 \tag{4.3}$$

It follows that the new values of σ_2 and σ_3, that is, their values at the surface following the glacial erosion to the depth h become:

$$\sigma_{2new} = \sigma_{3new} = \sigma_2 + \Delta\sigma_2 = \rho_r g h - \frac{\nu}{(1-\nu)}\rho_r g h \tag{4.4}$$

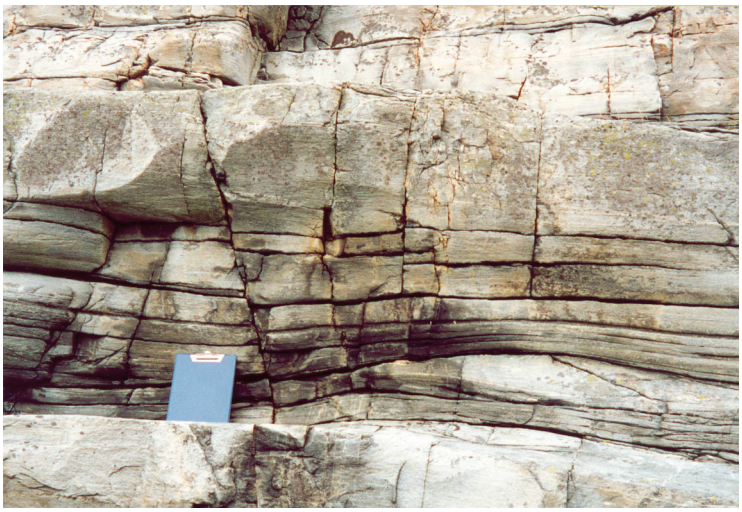

Figure 4.6: *Interconnected extension fractures in Øygarden, an island west of Bergen, Norway.*

The new principal stresses calculated from Equation (4.4) need no longer be the intermediate and minimum principal compressive stresses; because of stress rotation as a result of glacial erosion, one of them may actually be the maximum compressive stress.

This means that for erosion, h, of 1000 m in a crustal bedrock in Norway with density, ρ_r, of 2600 kgm^{-3}, the erosion-related horizontal compressive stress becomes 17 MPa. Thus this shows that erosion, or more generally, any removal of overburden (such as deglaciation, excavation or weathering and erosion) leads to surface parallel compressive stresses that can form or reactivate faults as reverse faults.

Horizontal compressive stresses may also result in the formation exfoliation fractures (Fig. 4.6), also called sheet joints, that is fractures developing parallel to the surface, which often can be seen in granites. The frequency of exfoliation fractures decrease rapidly with depth, but they will, if they become interconnected, contribute to the permeability at shallow crustal depths.

Clearly, erosion, or unloading, affects the stress field, and may, for large amounts of erosion, contribute positively to the permeability in an area.

The stress effect of erosion on petroleum reservoirs in the southwest Barents Sea is discussed in Paper F of this thesis.

Chapter 5

Numerical modelling

Modelling of stress, strain and displacement caused by applied loads on a material body with certain material properties are done by analytical or numerical calculations. Generally, analytical solutions can only be found in problems associated with simple geometries and small strains, and the body is assumed homogeneous and isotropic. When the problems become too complex to solve analytically, numerical models are used.

There are two categories of numerical methods of stress analysis, differential methods and integral methods (Brady and Brown, 1985). In differential methods, the problem is divided into a set of volumetric elements (3D), or surface elements (2D). The solution to the problem is obtained by using numerical approximations of the differential equations in each of the elements. The approximations are then combined into a solution of the entire material body. The finite element method (FEM) represents the differential method. In FEM models the problem domain is divided by a mesh of commonly triangular elements (Fig. 5.1). The nodes, where the unknown values are calculated during the modelling, are placed in the corners of each element. The commercial software COMSOL Multiphysics (www.comsol.com), used for modelling in Paper F of this thesis, is based on the FEM.

In the boundary element method (BEM), representing the integral method, solving the problem only requires a discretisation of the surface (Brebbia and Dominguez, 1992). The integration is performed over the boundary only, so the elements need to cover only the surface area as shown in Figure 5.2, instead of filling the volume as is necessary in FEM. Since the elements and nodes are placed at the boundary, the geometry can be followed exactly. Also, the solution for boundary problems (e.g. surface stresses) will be accurate using the BEM, while this is extrapolated in FEM. The software BEASY (www.beasy.com) used for the stress analysis in this thesis is based on the BEM.

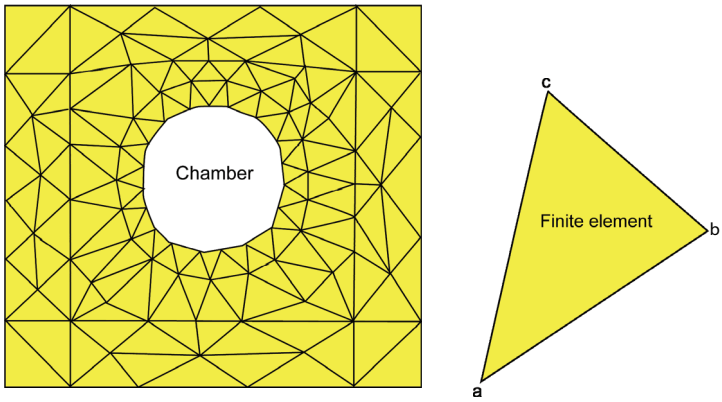

Figure 5.1: *A finite element model meshed by triangles.'Chamber' used here, refers to any type of a cavity; empty or filled with a fluid. In b) a single element with the nodes a, b and c is represented.*

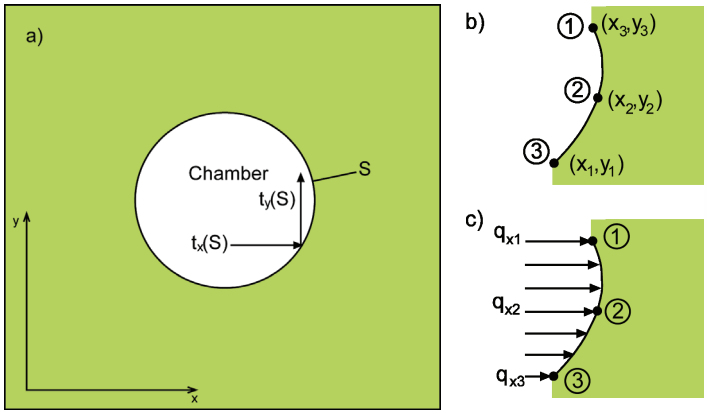

Figure 5.2: *A boundary element model with tractions on the surface S is shown in (a). An individual boundary element is represented by three nodes (b) subjected to load lines q_x and q_y (c), q_y is not shown. Modified from Brady and Brown (1985).*

5.1 Elastic properties

Most numerical software programs used for stress modelling in solid rocks are based on linear elasticity theory. In linear elastic materials, there is a linear relationship between stress and strain, that is, they follow Hooke's law:

$$\sigma = \epsilon E \tag{5.1}$$

where σ is the stress, ϵ the strain, and E is Young's modulus. Rocks normally behave linear elastic up to 1-3% strain at low temperature and pressure (Paterson, 1978; Farmer, 1983).

Linear elastic materials need to be described in terms of elastic parameters. For an isotropic material, whose response is independent of the orientation of the applied stress, numerous elastic parameters can be defined. The most common are Young's modulus (E), Poisson's ratio (ν), shear modulus (G), bulk modulus (K), and Lamè's constant (λ). However, only two of them are independent, so that if two of them are known the others can be derived. In stress modelling, the elastic parameters Young's modulus and Poisson's ratio are the ones normally used (Hudson and Harrison, 1997). Young's modulus is a measure of material stiffness, that is, the resistance against being compressed by uniaxial stress (Eq. 5.1).

Laboratory measurements, such as the uniaxial compression test, are used to determine the static Young's modulus of a rock specimen. These laboratory values tend to be higher than in-situ values (Goodman, 1989; Bell, 2000), due to the appearance of faults and fractures that lower the effective stiffness of an in-situ rock layer (Priest, 1993).

Rock types	Young's modulus, (GPa)
Unconsolidated sands	0.01 - 0.1
Sandstone	0.1 - 30
Clay	0.06 - 0.15
Shale	0.4 - 70
High Porosity Chalk	0.5 - 5
Low Porosity Chalk	5 - 30
Basalt	50 - 100
Granite	5 - 85
Marble	5 - 90
Ice	8

Table 5.1: *Static laboratory Young's modulus values for some common rocks types. From Fjær et al. (2008).*

Dynamic Young's modulus can be obtained from P and S-wave velocities (e.g. from seismic), however, these are normally used for processes of velocities like seismic waves (e.g. earthquakes). Because hydrofracture propagation is normally much slower than this, the static Young's modulus is the one commonly used. Table 5.1 shows the typical range of static Young's modulus of some common rock types.

The methods used for determining Young's modulus, also determine Poisson's ratio, which is a measure of lateral expansion in relation to longitudinal contraction.

$$\nu = -\frac{\epsilon_y}{\epsilon_x} \tag{5.2}$$

where ν is the Poisson's ratio ϵ_y and ϵ_x the lateral and longitudinal strain. Poisson's ratio for rocks is typically 0.15-0.35 (Fig. 5.3). In extreme cases values as high as 0.5 has been reported, these probably are related to highly anisotropic rocks (Gercek, 2007). Thermal induced microcracking in granites may cause negative Poisson's ratio in compression and tension (Homand-Etienne and Houpert, 1989). For the models presented in this thesis, the general value 0.25 is used for all rock types.

5.2 Boundary conditions

Generally, before starting the modelling the problem must be simplified so as to focus only on the details considered important. For example, many three dimensional problems may be reduced to two dimensions, if one of the dimensions can be regarded as infinite. A set up of a model includes defining the geometry, assigning elastic properties to the material under consideration, and specifying the loading conditions.

The geometry of the problem is described by means of points and lines (BEASY), or as a combination of pre-defined geometrical units (COMSOL). Hydrofractures with internal overpressures are normally modelled as mathematical cracks with zero opening, or as elliptical holes, as described in Chapter 3.2.

Fluid-filled reservoirs come in various dimensions and shapes. However, the shapes of petroleum reservoirs are commonly assumed to be crudely similar that of an oblate ellipsoid or a flat disk (Geertsma, 1973a,b; Segall, 1989; Zoback, 2007; Fjær et al., 2008). Such a geometry is a good first approximation to the actual reservoir geometry of petroleum reservoirs (Zoback, 2007; Fjær et al., 2008), as well as for magma chambers (Sneddon and Lowengrub, 1969). The latter may also be modelled as empty circular holes (Gudmundsson, 1998).

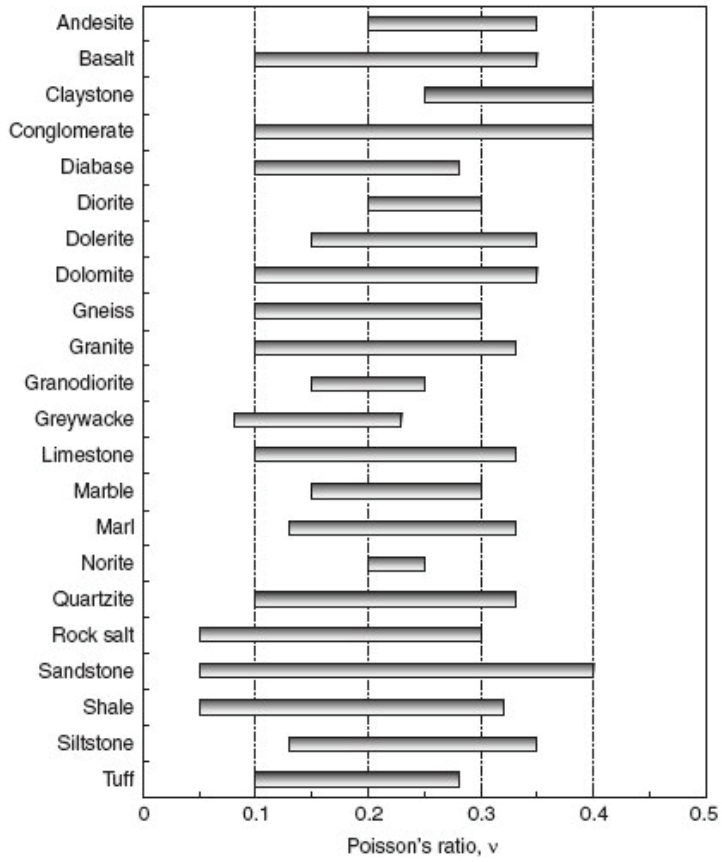

Figure 5.3: *Typical range of values for Poisson's ratio of some common rock types. From Gercek (2007).*

Conditions such as sliding surfaces and internal springs (the latter only available in BEASY) can be added to interfaces, to represent faults, fractures and other discontinuities. Another possibility is to model these features as empty narrow zones, or zones with low Young's modulus representing fault zones with gouge or breccia.

When realistic elastic properties (in accordance to Table 5.1) have been assigned to each department of the model, the load must be specified. The majority of numerical models in this thesis involve fluid overpressure, that is, either hydrofractures or fluid reservoirs. Since the fluid overpressure is determined by the

total fluid pressure minus the minimum compressive stress, it is crucial to examine the regional stress field in the area of consideration (cf. Chapter 4.2), so as to obtain a realistic model.

Before the model is run, it must be fastened in the corners to prevent rotation and translation.

5.3 Rock strength

The calculated stress in the resulting numerical model is based on the assumption of a linearly elastic material. However, the elastic behaviour of rocks depends on their rock strength, which is defined as the maximum applied compressive or tensile stress that the rock can withstand before failure occurs. The tensile strength of most solid rocks is in the range 0.5 to 6 MPa, most commonly 2-3MPa (Haimson and Rummel, 1982; Amadei and Stephansson, 1997). This means that crustal tensile stress exceeding these values is not very common, as it is likely to result in tensile failure of the rock. For this thesis, the numerical models are redrawn as to display a realistic maximum value of stress. Thus the tensile stress is normally truncated at 10 MPa. The shear strength of rocks is twice the tensile strength, as can be followed from the Griffith failure criterion (Jaeger et al., 2007), so that in the models, shear stress is truncated at subsequently higher values.

Chapter 6

Summary of papers

This chapter gives an overview of research papers included in the second part of this thesis. The following summaries present the main results as regards interpretation of field data, and the analytical and numerical modelling.

Paper A:

Propagation pathways and fluid transport of hydrofractures in jointed and layered rocks in geothermal fields.
Gudmundsson, A., Fjeldskaar, I. and Brenner, S. L., 2002.
Journal of Volcanology and Geothermal Research 116, 257-278.

Paper A focuses on the formation and propagation of hydrofractures in geothermal fields. Field data on current and extinct geothermal fields, mainly based on examination of networks of mineral veins in the Tertiary lava pile of North Iceland, are summarized in the first part of the paper. The data indicate that hydrofractures are common suppliers of fluids in these environments.

Next, we present boundary element models focusing on crack-tip tensile stresses and opening displacements of hydrofractures. The only loading in the models is the internal fluid overpressure of the hydrofracture, which varies linearly from 0 MPa at the tip to 10 MPa at its centre. In the majority of the presented models the host rock has a uniform stiffness (Young's modulus 10 GPa and Poisson's ratio 0.25) with vertical and horizontal discontinuities, modelled as internal springs of 6 MPa/m, representing columnar joints and contacts between lava flows. The size and location of the discontinuities, and the location of the hydrofracture tip, vary between the models. The results from the numerical modelling show that the resulting crack-tip tensile stresses are high enough to open and link up discontinuities in the layered and jointed rock masses ahead of the propagating hydrofracture (Figure 6.1).

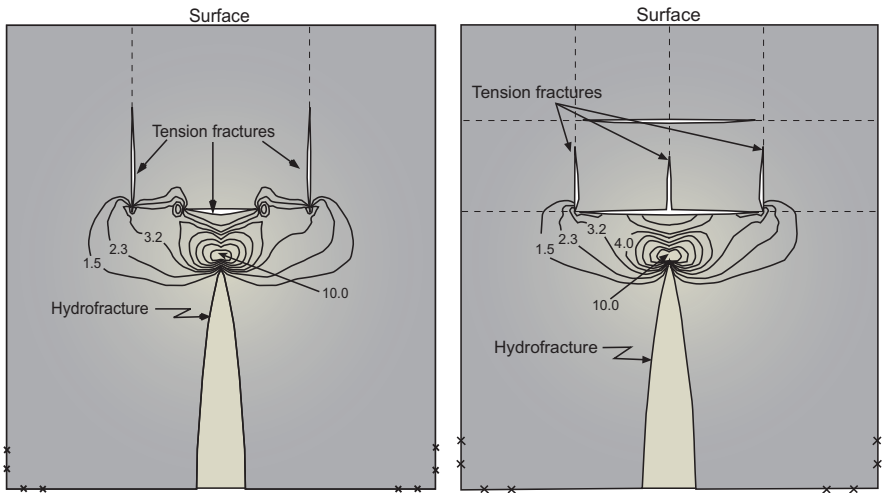

Figure 6.1: *Boundary-element models showing how the crack-tip tensile stresses associated with a propagating hydrofracture open up both vertical and horizontal discontinuities. The tensile stresses are given in MPa.*

In the last part of the paper, we present analytical models on fluid flow along vertical and inclined hydrofracture pathways, to estimate the dimensions of a hydrofracture network necessary to supply typical hot springs with the measured volumetric rates. The analytical models indicate that a hot spring yielding 5 l/s may be supplied by a hydrofracture of aperture 1.3 mm and trace length 0.5 m, similar to those of the most common mineral veins in the studied palaeogeothermal field. The primary driving force of hydrofractures in such fields appears to be buoyancy.

Paper B:

Fracture-generated permeability and groundwater yield in Norway.
Gudmundsson, A., Fjeldskaar, I. and Gjesdal, O., 2002.
NGU Bulletin 439, 61-69.

In paper B, we have focused on the bedrock hydrogeology of Norway. In Norway, there is observed a linear relationship between the current postglacial uplift rates and groundwater yield. The groundwater transport in bedrock is largely determined by the interconnection of fractures, thus the conditions that favour fracture propagation and interconnection is of major importance when it comes to understanding the permeability and ground water yield in Norway.

Figure 6.2: *Extension fractures linked up through transverse shear fractures in Øygarden. View is south-southwest; the length of the steel tape is 1.5 m.*

First, we present some field examples of small scale fracture systems as indications of permeability development.The examples are from Øygarden, an island west of Bergen in the western part of Norway. Next, we present boundary element models, where the focus is on propagation of two types of fractures; extension fractures (hydrofractures) and shear fractures. The first model shows two offset fractures, modeled as internal springs of 6 MPa/m, in a homogeneous host rock (Young's modulus 10 GPa, and Poisson's ratio 0.25) subject to horizontal tensile stress of 6MPa. The result indicates that the offset fractures may link up by transverse shear fractures to form an interconnected system of en echelon segments,

as shown in Figure 6.2. The next boundary element models show the propagation of a hydrofracture through linking up with vertical and horizontal discontinuities ahead of its tip, similar to the models shown in Paper A. The last two models are of a hydrofracture approaching a soft layer (Young's modulus 5 GPa and Poisson's ratio 0.25) with two vertical joints of stiffness 6 MPa/m and length 0.4 units reaching the surface. The result shows that the crack-tip tensile stresses of the propagating hydrofracture are high enough to open up the vertical joints all the way to the surface.

The data and modeling results indicate that the rapid erosion and postglacial uplift are likely to have generated stress fields suitable for the linking up and growth of interconnected fracture systems in parts of Norway.

Paper C:

Effects of linking up of discontinuities on fracture growth and groundwater transport.
Gudmundsson, A., Gjesdal, O., Brenner, S. L. and Fjeldskaar, I., 2003.
Hydrogeology Journal 11, 84-99.

Paper C deals with the effects of fracture growth on the generation and maintenance of permeability in solid rock. The emphasis is on groundwater reservoirs (Fig. 6.3), where the permeability of the associated fracture networks largely controls the groundwater flow; however, the results may also have implications for permeability of other fluid reservoirs.

Field data, primarily collected from Iceland, England and Norway, on the two types of tectonic fractures, that is, extension fractures (tension fractures and hydrofractures) and shear fractures (faults), is summarized and discussed in the first part of the paper.

Next, we consider two mechanisms that may lead to interconnection of discontinuities: external tensile stress and internal fluid overpressure (hydrofractures). Several boundary element models are developed and presented in this paper. The boundary element models on the propagation of hydrofractures through linking up of discontinuities are similar to the ones presented in paper A. The next models show en echelon systems of sets of extension-fracture segments in a host rock of uniform stiffness (with Young's modulus of 10 GPa and Poisson's ratio of 0.25) subject to an erosion-related horizontal tensile stress of 6 MPa. The distance between the extension fractures vary, both parallel to (underlapping) and perpendicular to (offset) the main trend of the segmented fracture.

The results show that for a significant underlapping, interconnection of shear fractures are favoured, whereas the collinear extension fractures favour tensile stresses and the growth of extension fractures into a single, segmented fracture.

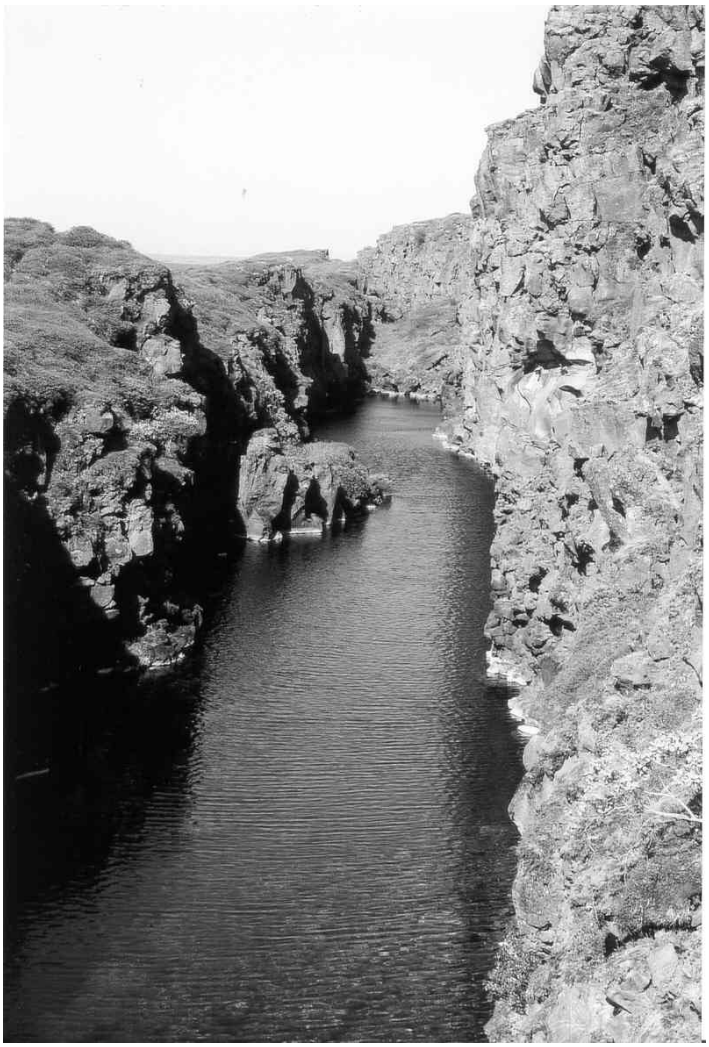

Figure 6.3: *A normal fault conducting groundwater in a pahoehoe lava flow in the Krafla Fissure Swarm in North Iceland. View northeast. Field observations indicate an opening of as much as 10 m, and a groundwater depth of tens of meters.*

The last part of this paper presents a boundary element model of an aperture variation of a hydrofracture subject to constant overpressure in a layered host rock, and this is compared with analytical models on the elliptical aperture variation of a hydrofracture in a homogeneous, isotropic host rock.

Paper D:

Dyke emplacement in a layered and faulted rift zone.
Gudmundsson, A. and Loetveit, I. F., 2005.
Journal of Volcanology and Geothermal Research Special Issue 144, 311-327.

Paper D deals with the effects of crustal layering and existing normal faults on the emplacement of dykes. In the first part of the paper we present field data on dykes and faults in layered rift zones from Tenerife (Canary Islands) and Iceland.

Next, we present three sets of boundary element models. In the first set of models, a vertical dyke with a constant magmatic overpressure of 10 MPa propagates through a uniform crust with Young's modulus of 10 GPa and Poisson's ratio of 0.25, and on its way towards the surface it approaches and passes the two boundary faults of a buried graben. The results show that the dyke tip tensile stresses tend to open up the faults as long as the magma front is below the lower tips of the faults, but as soon as the magma front reaches the level of the lower fault tips the faults close and then slip as reverse faults.

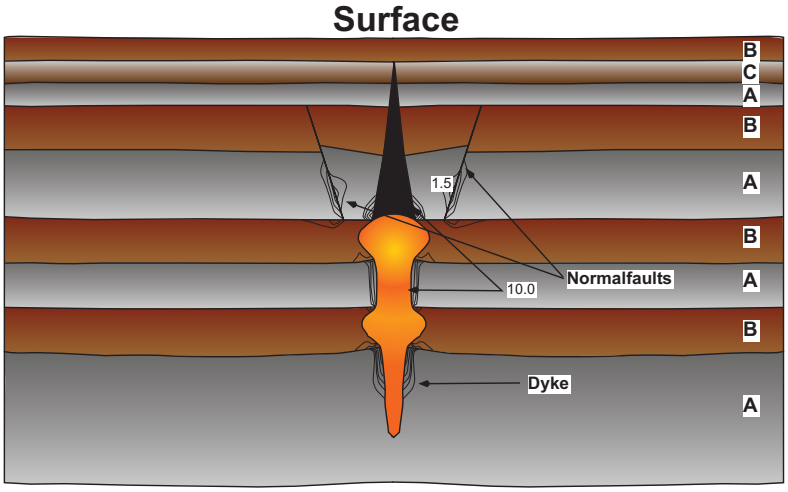

Figure 6.4: *Boundary-element model of a propagating dyke in a layered and faulted rift zone. The A layers are very stiff, the B layers are very soft and the C layer is moderately stiff. The only loading in the model is the magmatic overpressure of 10 MPa inside the dyke. The results shows that when the magmafront is at the same level as the lower tips of the faults, the overpressure induce reverse slip on the faults. The dyke aperture is largest in the soft B layers.*

In the second set of models, a dyke approaches and passes a buried graben in a host rock composed of nine layers (Fig. 6.4). There are three types of mechanical layers, varying in Young's modulus between 100 GPa (stiff layers), 5 GPa (soft layers) and 10 GPa (moderately soft layers). Poisson's ratio is 0.25 for all the layers. The models show the same results as for the previous models (homogeneous crust models), as regards the opening and reverse slip of the faults, but in addition these models show effects of layer stiffness on the dyke aperture. The thickest parts of the dyke tend to be in the soft layers.

In the last set of models, a dyke with linearly varying overpressure from 10 MPa at the bottom of the model to 0 Mpa at the magma front is arrested at 1 km below the surface. Above the magma front the crust consist of two layers of thickness 0.4 km; the soft layer B (5 GPa) and a relatively stiff surface layer A (40 GPa). In the first model, both the layers are subject to a horizontal compression that increases linearly from 0 MPa at the surface, to 20 MPa at 0.8 km depth. The results show no stress effect at the surface. In the second model the B layer has a high stiffness of 100 GPa, and a weak contact on the lower B layer boundary at 0.8 km is included. Although the dyke tip tensile stresses reaches 111 MPa, no stress is transferred to the surface.

Paper E:

Propagation, deflection, arrest and shape of hydrofractures in heterogeneous rocks.

Løtveit, I. F., Gudmundsson, A. and Philipp, S. L.

To be submitted.

In Paper E the focus is on the effects of mechanical layering on the propagation and arrest of hydrofractures. In the first part of the paper we review and summarise data on reservoirs and their main fracture types.

Next, we present some analytical models on the initiation, propagation, deflection and shape of hydrofractures. The presented analytical models on hydrofracture initiation and propagation indicate that for any significant fluid overpressure, hydrofractures in a homogeneous, isotropic reservoir rarely should become deflected or arrested. By contrast, when a hydrofracture meets discontinuities such as a contact or an existing fracture, the hydrofracture may either become arrested, become deflected along the contact, or continue its propagation into the contact. Here, three related factors are explored. They are (1) the induced tensile stress ahead of the propagating hydrofracture tip, (2) the rotation of the principal stresses at the discontinuity and (3) the elastic mismatch and the difference in material toughness between the contact and the adjacent rock. The results suggest that

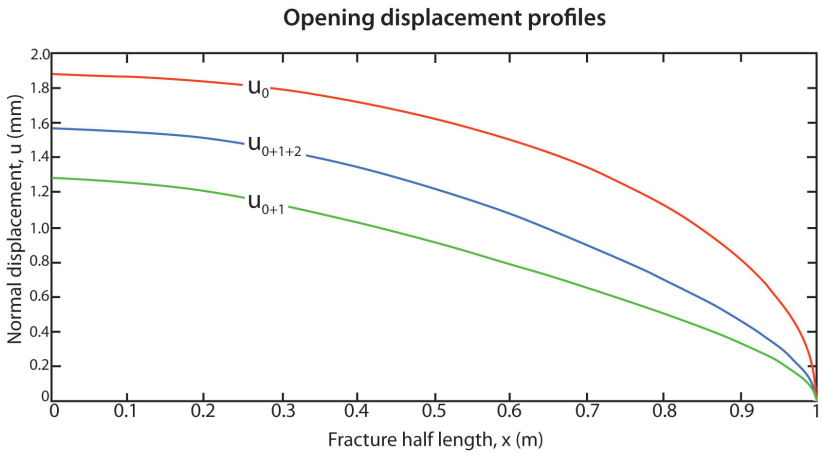

Figure 6.5: *Opening displacement profiles resulting from constant (u_0), linearly(u_{0+1}) and polynomially (u_{0+1+2}) varying fluid overpressure.*

contacts where the hydrofracture propagates from a stiff layer to a soft layer have little effects on the propagation pathway. By contrast, contacts where the hydrofracture propagates from a soft into a stiff layer encourage deflection and/or arrest.

In the last part of the paper we present some analytical and numerical models on the opening displacement of a hydrofracture. For a hydrofracture propagating in a homogeneous host rock, the analytical solutions show that constant, linearly and polynomially varying fluid overpressure all result in similar aperture shapes, but the sizes are somewhat different (Fig. 6.5). However, when the host rock is layered, the aperture tends to be larger in the soft layers. Large aperture variations encourage flow channelling.

Paper F:

Effects of glacial erosion on the state of stress and fluid pressure in petroleum reservoirs in the Barents Sea.
Løtveit, I. F., Gudmundsson, A., Leknes, L., Riis, F. and Fjeldskaar, W.
Submitted to Journal of Geological Society.

In Paper F we focus on the Late-Pliocene-Pleistocene glacial erosion in the southwest part of the Barents Sea and the associated stress effects, particularly as regards fluid pressure changes inside, and potential leakage of, petroleum reservoirs in this area. In the first part of the paper, we present basin modeling results

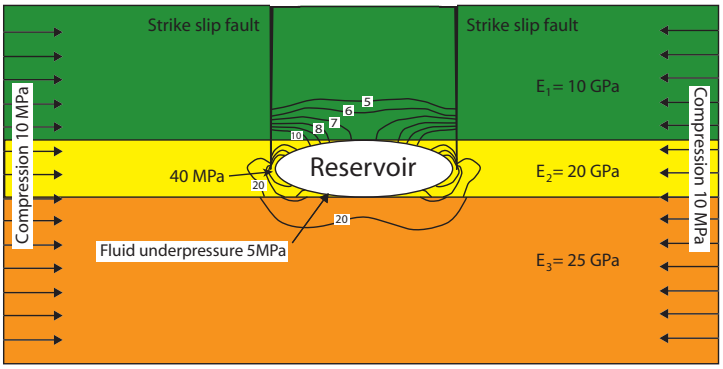

Figure 6.6: *Numerical model showing the von Mises shear stress (in mega-pascals) around a small reservoir subject to fluid underpressure of 5 MPa and, simultaneously, horizontal compressive stress of 10 MPa. The resulting shear stress is concentrating near to the tips of the strike slip faults, indicating that the faults are likely to be reactivated. Maximum stress shown is 40 MPa.*

on the amount of erosion in the southwestern Barents Sea. The results suggest a glacial erosion of 900 m for the Hammerfest Basin (Snøhvit), 1300m for the Loppa High, and 1100 m for the Finnmark Platform.

The second part of the paper deals with the stress effects of erosion on the reservoirs at Loppa High and Snøhvit. First, we present analytical models on the changes in crustal stress due to the unloading of sediments. These analytical models show that a rapid removal of 900m and 1300m of sediments result in a horizontal compressive stresses of magnitude 11.5 MPa and 17 MPa, respectively. The resulting erosion-related compressive stress is calculated at the new surface, below the surface the compression is expected to be somewhat lower. The new surface consists of sedimentary rocks that are unconsolidated, thus the Young's modulus is very low. It follows that the compressive stress tends to be suppressed in the upper unconsolidated layer, whereas it will tend to concentrate in the stiff layers below.

The Snøhvit reservoirs are situated in a Jurassic sand formation acting as an unconfined salt water aquifer. The modelled reservoirs refer to the accumulation of oil and gas in this aquifer. Normally, gas responds to compression by expanding, but since it is trapped between the low permeable shale layer at the roof of the reservoir and the oil at the lower part of the reservoir, the result is an overpressured gas. Analytical tunnel-crack and elliptical plate-bending models show that the erosion-related horizontal compression may have influenced the reservoir fluid pressure by first lead to overpressure and expansion, then to fluid underpressure

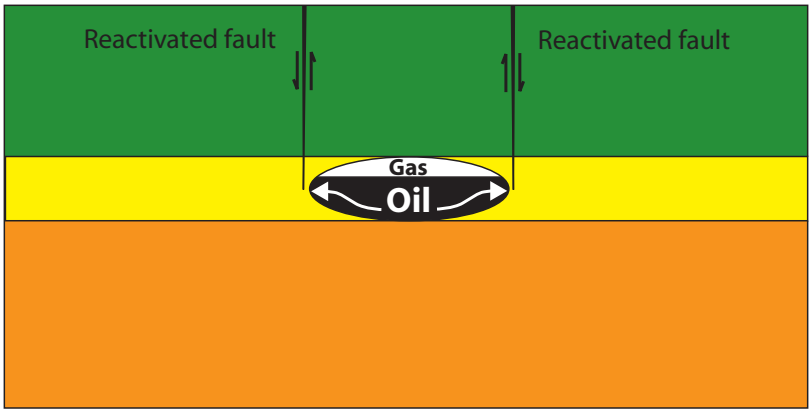

Figure 6.7: *In a reservoir, the gas normally accumulate on top of the oil, due to its much lower density. Reactivation and increased permeability of faults close to the lateral ends of reservoir with a cross-section similar to an ellipse may offer paths for oil but unlikely to offer paths for the gas.*

as a consequence of the reservoir expansion.

In the last part of the paper we present several numerical models on the stress effects of erosion on a fluid reservoir and its nearby faults. In all the models, the reservoir is modeled as an ellipse in layered host rock, with faults extending from its lateral ends to the surface. The first model is of a small fluid reservoir subject to a fluid overpressure of 5 MPa with normal faults close to its lateral ends. The result shows that the shear stress near to the ends of the faults exceeds 40 MPa, indicating that the normal faults are likely to be reactivated as reverse faults. The shear stress also concentrates at the lateral ends of the reservoir, indicating that the reservoir is likely to expand laterally. The expansion of the reservoir will lead to an increase in volume, which in turn leads to lowering of the fluid pressure giving rise to a possible underpressure. The next model is very similar, except this time the reservoir is subject to a fluid underpressure and the faults are now reverse faults. The result shows a slight subsidence of the block above the reservoir, and high shear stresses near to the tip of the faults, indicating a likely reactivating of the reverse faults. The same results is shown for the next models, which show strike slip faults near to a reservoir subject to a horizontal compression of 10MPa, and strike slip faults near to a reservoir subject to a fluid underpressure of 5 MPa and a horizontal compression of 10 MPa, as shown in Figure 6.6. All the numerical models suggest that any faults (normal, strike-slip, and reverse) close to the lateral ends of the reservoirs are likely to have been reactivated as a result of the glacial erosion in the Barents Sea. Figure 6.7 shows

what we suggest may be, at least partly, the explanation for an overall abundance of gas and the leakage of moveable oil in the southwestern Barents Sea reservoirs.

Currently, there are no proofs of oil leakage along the faults in the Snøhvit area. However, this may be caused by the fact that major fault zones are avoided during drilling. Also, seismic data shows no sign of reactivation of the large faults from normal to reverse faults. The faults in this area are suggested to be significantly older than the erosion. However, seismic data normally have a resolution of 10-12 m, so that a fault displacements less than this are not seismically visible. Previous field observations in an area with similar magnitude of horizontal crustal compression indicated a displacement of a few meters (Gudmundsson et al., 2008). In the Barents Sea area this would imply that the normal faults would experience a displacement that reverses the normal movement by a few meters.

Chapter 7

Conclusions

1. Fluid flow in solid rocks is commonly largely, or entirely, controlled by interconnected fractures. There are two basic ways by which fractures become interconnected. One is through the development of shear fractures, that is, faulting. The other is through the propagation of overpressured, fluid-filled fractures, referred to as hydrofractures.

2. Hydrofractures are among the most common brittle structures in the Earth's crust and include many dykes, sills, mineral-filled veins, man-made hydraulic fractures (used in petroleum engineering to increase reservoir permeability) and many joints. In addition, hydrofractures play a significant role in seismogenic faulting and associated hydraulic changes. The importance of propagating hydrofractures on the development of interconnected fracture pathways for fluids is emphasized and explained.

3. Many numerical models, using the boundary-element program BEASY and the finite-element program COMSOL, were made to study the condition for propagation of hydrofractures. Particular attention was given to the conditions of hydrofracture arrest, as well as those for hydrofracture propagation through the linking up of horizontal and vertical discontinuities in jointed and layered rock masses. The results of the numerical models show that for a homogeneous host rock the crack-tip tensile stresses associated with propagating hydrofractures are large enough to open up discontinuities far ahead of the fracture tip. This applies both to the vertical discontinuities as well as to horizontal discontinuities. Tensile stress concentrations at the tips of the opened-up discontinuities indicate that they would tend to propagate and coalesce into an interconnected fracture pathway.

4. Numerical modelling on the effects of mechanical layering show that when fluid pressure is the only loading, stiff layers tend to magnify the crack-tip

tensile stresses associated with a propagating hydrofracture, and therefore encourage hydrofracture propagation. By contrast, soft layers tend to suppress the crack-tip tensile stresses of the propagating hydrofracture, and thereby encourage hydrofracture arrest. These results are supported by hydraulic fracture experiments in petroleum engineering (Valko and Economides, 1995; Yew, 1997).

5. The numerical models show that mechanical layering also affects the aperture variations of hydrofractures. For a vertical hydrofracture, the aperture is normally greater in soft layers than in stiff layers. Similar results have been obtained in other numerical models (Gudmundsson and Brenner, 2001a,b). Aperture variations may lead to flow channeling, that is, preferential flow in layers with the mechanical properties most optimal for flow.

6. All the model results indicate that, for a layered rock mass, it is generally easier for a hydrofracture to enter a stiff than a soft layer because the tensile stresses associated with the hydrofracture tip are larger in a stiff than in a soft layer. For vertical discontinuities such as joints ahead of the hydrofracture tip, however, the resulting apertures and dip dimensions (heights) become smaller when they are hosted by a stiff than by a soft layer.

7. Numerical models indicate that there is an interaction between a propagating hydrofracture and fault slip in a layered host rock. Boundary-element models of a hydrofracture propagating into a graben of two normal faults show that crack tip tensile stresses associated with a hydrofracture propagating towards the bottom parts of the graben tend to reduce the normal stresses on the boundary faults. When the hydrofracture tip reach the same level as the lowermost parts of the faults, however, its associated tensile stress tend to close the faults, and encourage reverse slip as it propagates further into the graben.

8. The numerical and theoretical models presented in this thesis indicate that the propagation and pathway formation of hydrofractures is a complex process. For hydrofractures emplaced in a layered and jointed rock mass, mechanical layering and discontinuities have strong effects on the probability of hydrofracture propagation or, alternatively, hydrofracture arrest. In particular, stress barriers, soft layers and horizontal discontinuities at layer contacts tend to encourage hydrofracture arrest, whereas absence of stress barriers, horizontal discontinuities and stiff layers tend to encourage hydrofracture propagation.

9. Modeling results indicate that rapid erosion and postglacial uplift are likely to have generated stress fields suitable for the linking up and growth of in-

terconnected fracture systems in parts of Norway. It is expected that during the deglaciation and erosion the crust was subject to temporary tensile stress fields, which may have significantly affected the permeability.

10. The western Barents Sea have experienced significant erosion over the last 3 million years. Analytical models indicate that erosion leads to crustal compression. Removal of 900 m of sedimentary rock, as is suggested for the Snøhvit area, with rock densities of 1950 kgm^{-3}, results in a horizontal compressive stress in the order of 17 MPa. Thus, erosion of this amount can produce compressive stresses that are likely to generate or reactivate faults as reverse faults.

11. Numerical models on fluid reservoirs (e.g. petroleum at Loppa High and Snøhvit) subject to erosion-generated compression show that shear stress tends to concentrate near to the ends of the reservoir. The shear stress in this area generated by compression of 15 MPa exceeds 40 MPa, indicating that faults near to the ends of the reservoirs are very likely to be generated or reactivated.

12. All numerical models suggest that any faults close to lateral ends of a petroleum reservoir in the southwest Barents Sea are likely to have been reactivated as a result of the rapid glacial erosion the last 3 Ma. This may at least partly explain the overall abundance of gas, and lack of commercial oil in the southwest Barents Sea.

13. It is shown that there are several factors affecting the fracture-generated permeability of rocks. The way hydrofractures and faults link up into networks, and their ability to be conduits for fluids, are largely determined by mechanical layering and the current stress field.

Part II

Papers

References

Acocella, V., Gudmundsson, A., Funiciello, R. 2000. Interaction and linkage of extension fractures and normal faults: examples from the rift zone of Iceland. *Journal of Structural Geology* **22**, 1233-1246.

Aguilera, R. 1995. *Naturally Fractured Reservoirs*. PennWell Publishing Company, Tulsa, Oklahoma.

Amadei, B., Stephansson, O. 1997. *Rock Stress and its Measurement*. Chapman & Hall, London.

Angelier, J., Slunga, R., Bergerat, F., Stefansson, R., Homberg, C. 2004. Perturbation of stress and oceanic rift extension across transform faults shown by earthquake focal mechanisms in Iceland. *Earth and Planetary Science Letters* **219**, 271-284.

Angelier, J. 1984. Tectonic analysis of fault slip data sets. *Journal of Geophysical Research* **89**, 5835-5848.

Atkins, A.G., Mai, Y.W. 1985. *Elastic and Plastic Fracture*. Horwood, Chichester.

Atkinson, B.K. 1987. *Fracture mechanics of rock*. Academic Press, London.

Baer, G. 1991. Mechanisms of dike propagation in layered rocks and in massive, porous sedimentary rocks. *Journal of Geophysical Research* **96**, 11911-11929.

Barton, C.A., Zoback, M.D., Moos, D. 1995. Fluid flow along potentially active faults in crystalline rock. *Geology* **23**, 683-686.

Bear, J. 1993. Modelling flow and contaminant transport in fractured rocks. In: Bear, J., Tsang, C.F., de Marsily, G. (eds). *Flow and Contaminant Transport in Fractured Rock*. Academic Press, New York, 1-37.

Bell, F.G. 2000. *Engineering Properties of Soils and Rocks*. Blackwell, Oxford.

Berglund, L.T., Augustson, J., Færseth, R.B., Gjelberg, J., Ramberg-Moe, H. 1986. The evolution of the Hammerfest Basin. In: Spencer, A.M. (ed.) *Habitat of Hydrocarbons on the Norwegian Continental Shelf*. Graham & Trotman, London, 319-338.

Bjørlykke, K., Ramm, M., Saigal, G.C. 1989. Sandstone diagenesis and porosity modification during basin evolution. *Geologische Rundschau* **78**, 243-268.

Bonafede, M., Rivalta, E. 1999a. On tensile cracks close to and across the interface between two welded elastic halfspaces. *Geophysical Journal International* **138**, 410-434.

Bonafede, M., Rivalta, E. 1999b. The tensile dislocation problem in a layered elastic medium. *Geophysical Journal International* **136**, 341-356.

Braathen, A., Berg, S.S., Storro, G., Jaeger, O., Henriksen, H., Gabrielsen, R. 1999. *Fracture -zone geometry and groundwater flow; results from fracture studies and drill tests in Sunnfjord*. Geological Survey of Norway, Report 99.017 (in Norwegian).

Brady, B.H.G., Brown, E.T. 1985. *Rock Mechanics for Underground Mining*. Allen & Unwin, London.

Brebbia, C.A., Dominguez, J. 1992. *Boundary Elements: an Introductory Course*. Computational Mechanics, Boston.

Broberg, K.B. 1999. *Cracks and Fracture*. Academic Press, London.

Brudy, M., Kjørholt, H. 2001. Stress orientation on the Norwegian continental shelf derived from borehole failures observed in high-resolution borehole imaging logs. *Tectonophysics* **337**, 65-84.

Bruhn, R.L., Parry, W.T., Yonkee, W.A., Thompson, T. 1994. Fracturing and hydrothermal alteration in normal fault zones. *Pure and Applied Geophysics* **142**, 609-644.

Bungum, H., Alsaker, A., Kvamme, L.B., Hansen, R.A. 1991. Seismicity and seismotectonics of Norway and nearby continental shelf areas. *Journal of Geophysical Research* **96**, 2249-2265.

Byrkjeland, U., Bungum, H., Eldholm, O. 2000. Seismotectonics of the Norwegian continental margin. *Journal of Geophysical Research* **105**, 6221-6236.

Caine, J.S., Evans, J.P., Forster, C.B. 1996. Fault zone architecture and permeability structure. *Geology* **24**, 1025- 1028.

Cartwright, J.A., Trudgill, B.D., Mansfield, C.S. 1995. Fault growth by segment linkage - An explanation for scatter in maximum displacement and trace length data from the Canyonlands Grabens of SE Utah. *Journal of Structural Geology* **17**, 1319-1326.

Cavanagh, A.J., Di Primio, R., Scheck-Wenderoth, M., Horsfield, B. 2006. Severity and timing of Cenozoic exhumation in the southwestern Barents Sea. *Journal of the Geological Society*, London **163**, 761-774.

Charlez, P.A. 1997. *Rock Mechanics, Volume 2: Petroleum Applications*. Editions Technip, Paris.

Cook, J., Gordon, J.E. 1964. A mechanism for the control of crack growth in all-brittle systems. *Proceedings of the Royal Society of London* **A282**, 508-520.

Domenico, P.A., Schwartz, F.W. 1998. *Physical and Chemical Hydrogeology*. Wiley, New York.

Engelder, T. 1993. *Stress Regimes in the Lithosphere*. Princeton University Press, New Jersey.

Evans, J.P., Forster, C.B., Goddard, J.V. 1997. Permeability of fault-related rocks, and implications for hydraulic structure of fault zones. *Journal of Structural Geology* **19**, 1393-1404.

Farmer, I. 1983. *Engineering Behaviour of Rocks*. Chapman & Hall, London.

Faulkner, D.R., Mitchell, T.M., Healy, D., Heap, M.J. 2006. Slip on 'weak' faults by the rotation of regional stress in the fracture damage zone. *Nature* **444**, 922-925.

Faybishenko, B., Witherspoon, P.A., Benson, S.M. (eds). 2000. *Dynamics of Fluids in Fractured Rocks*. Washington DC.

Finkbeiner, T., Barton, C.A., Zoback, M.D. 1997. Relationships among in-situ stress, fractures and faults, and fluid flow: Monterey formation, Santa Maria basin, California. *American Association of Petroleum Geologists Bulletin* **81**, 1975-1999.

Fjær, E., Holt, R.M., Horsrud, P., Raaen, A.M., Risnes, R. 2008. *Petroleum Related Rock Mechanics*, 2nd ed. Elsevier, Amsterdam.

Fjeldskaar, W., 1997. Flexural rigidity of Fennoscandia inferred from the postglacial uplift. *Tectonics* **16**, 596-608.

Fjeldskaar, W., Lindholm, C., Dehls, J.F., Fjeldskaar, I. 2000. Post-glacial uplift, neotectonics and seismicity in Fennoscandia. *Quaternary sciencce Reviews* **19**, 1413-1422.

Geertsma, J. 1973a. A basic theory of subsidence due to reservoir compaction: the homogeneous case. *Verhandelingen Kon. Ned. Geol. Mijnbouwk Gen.* **28**, 43-62.

Geertsma, J. 1973b. Land subsidence above compacting oil and gas reservoirs. *Journal of Petroleum Technology* **25**, 734-744.

Gercek, H. 2007. Poisson's ratio values for rocks. *International Journal of Rock Mechanics & Mining Sciences* **44**, 1-13.

Gillespie, P.A., Walsh, J.J., Watterson, J., Bonson, C.G., Manzocchi, T. 2001. Scaling relationships of joint and vein arrays from The Burren, Co Clare, Ireland. *Journal of Structural Geology* **23**, 183-201.

Goodman, R.E. 1989. *Introduction to Rock Mechanics*, 2nd ed. Wiley, New York.

Gudmundsson, A., Brenner, S.L. 2001. How hydrofractures become arrested. *Terra Nova* **13**, 456-462.

Gudmundsson, A., Berg, S.S., Lyslo, K.B., Skurtveit, E. 2001. Fracture networks and fluid transport in active fault zones. *Journal of Structural Geology* **23**, 343-353.

Gudmundsson, A., Friese, N., Galindo, I., Philipp, S.L. 2008. Dyke-induced reverse faulting in a graben. *Geology* **36**, 123-136.

Gudmundsson, A. 1990. Emplacement of dikes, sills and crustal magma chambers at divergent plate boundaries. *Tectonophysics* **176**, 257-275.

Gudmundsson, A. 1992. Formation and growth of normal faults at the divergent plate boundary in Iceland. *Terra Nova* **4**, 464-471.

Gudmundsson, A. 1998. Magma chambers modeled as cavities explain the formation of rift zone central volcanoes and their eruption and intrusion statistics. *Journal of Geophysical Research* **103**, 7401-7412.

Gudmundsson, A. 1999. Postglacial doming, stresses and fractures formation with application to Norway. *Tectonophysics* **307**, 407-419.

Gudmundsson, A. 2000a. Fracture dimensions, displacements and fluid transport. *Journal of Structural Geology* **22**, 1221-1231.

Gudmundsson, A. 2000b. Active fault zones and groundwater flow. *Geophysical Research Letters*, **27**, 2993-2996.

Gudmundsson, A. 2000c. Dynamics of volcanic systems in Iceland: Example of tectonism and volcanism at juxtaposed hot spot and mid-ocean ridge systems. *Annual Review of Earth and Planetary Sciences* **28**, 107-140.

Gudmundsson, A., 2001: Fluid overpressure and flow in fault zones: field measurements and models. *Tectonophysics* **336**, 183-197.

Gudmundsson, A. 2002. Emplacement and arrest of sheets and dykes in central volcanoes. *Journal of Volcanology and Geothermal Research* **116**, 279-298.

Gudmundsson, A. 2004. Effects of Young's modulus on fault displacement. *C.R. Geoscience* **336**, 85-92.

Haimson, B.C., Rummel, F. 1982. Hydrofracturing stress measurements in the Iceland research drilling project drill hole at Reydarfjördur, Iceland. *Journal of Geophysical Research* **87**, 6631-6649.

Haneberg, W.C., Mozley, P.S., Moore, J.C., Goodwin, L.B. (eds). 1999. *Faults and Subsurface Fluid Flow in the Shallow Crust*. American Geophysical Union, Washington DC.

Heap, M.J., Faulkner, D.R. 2008. Quantifying the evolution of static elastic properties as crystalline rock approaches failure. *International Journal of Rock Mechanics & Mining Sciences* **45**, 564-573.

Heidbach, O., Tingay, M., Barth, A., Reinecker, J., Kurfeß, D., Müller, B. 2008. The 2008 release of the World Stress Map (available online at www.world-stress-map.org).

Heimpel, M., Olson, P. 1994. Buoyancy-driven fracture and magma transport through the lithosphere: models and experiments. In: Ryan, M.P. (ed.). *Magmatic Systems*. Academic Press, London, 223-240.

Hicks, E.C., Bungum, H., Lindholm, C. 2000. Stress inversion of earthquake focal mechanism solutions from onshore and offshore Norway. *Norsk Geologisk Tidsskrift* **80**, 235-250.

Homand-Etienne F, Houpert R. 1989. Thermally induced microcracking in granites: characterization and analysis. *International Journal of Rock Mechanics & Mining Sciences Geomechanical Abstract* **26**, 25-34.

Hudson, J.A., Harrison, J.P. 1997. *Engineering Rock Mechanics: an Introduction to the Principles*. Pergamon, Oxford.

Iliffe, J.E., Robertson, A.G., Ward, G.H.F., Wynn, C., Pead, S.D.M., Cameron, N. 1999. The importance of fluid pressures and migration to the hydrocarbon prospectivity of the Faeroe-Shetland While Zone. In: Fleet, A.J., Boldy, S.A.R. (eds). *Petroleum Geology of Northwest Europe* **1**. Geological Society of London, 601-611.

Jaeger, J.C., Cook, N.G.W. 1979. *Fundamentals of Rock Mechanics*. Chapman & Hall, London.

Jaeger, J.C., Cook, N.G.W, Zimmerman, R.W. 2007. *Fundamentals of Rock Mechanics*. Chapman & Hall, London. 2nd ed.

Kim, K., Franklin, J.A. 1987. Suggested methods for rock stress determination. *International journal for Rock Mechanics and Mining Sciences* **24**(1), 53-74.

Kusumoto, S., Gudmundsson, A. 2009. Displacement and stress fields around rock fractures opened by irregular overpressure variations given by Fourier cosine series. *Submitted*.

Lee, C.H., Farmer, I.W. 1993. *Fluid flow in Discontinuous Rocks*. Chapman and Hall.

Linjordet, A., Grung-Olsen, R. 1992. The Jurassic Snøhvit Gas Field Hammerfest Basin, Offshore Northern Norway. In: Halbouty, M.T. (ed.). Giant Oil and Gas Fields of the Decade 1978-1988. *American Association of Petroleum Geologists, Memoirs*, **54**, 349-370.

Marinoni, L.B., Gudmundsson, A. 2000. Dyke, faults and paleostresses in the Teno and Agana massifs of Tenerife (Canary Islands). *Journal of Volcanology and Geothermal Research* **103**, 83-103.

Maugis, D. 2000. *Contact, Adhesion and Rupture of Elastic Solids*. Springer, Berlin.

McClay, K.R. 1987. *The Mapping of Geological Structures*. John Wiley & Sons, Chichester.

Morland, G. 1997. Petrology, lithology, bedrock structures, glaciation and sea level. Important factors for groundwater yield and composition of Norwegian bedrock boreholes? *Geologcial Survey of Norway Report* 97.122 I.

Mörner, N.A. 1980. The Fennoscandian uplift: geological data and their geodynamic implications. In: Mörner, N.A. (Ed.), *Earth Rheology, Isostacy and Eustacy*. Wiley, New York, 251-284.

Nelson, R.A. 1985. *Geologic Analysis of Naturally Fractured Reservoirs*. Gulf Publishing, Houston, Texas.

Nunn, J.A., Meulbroek, P. 2002. Kilometer-scale upward migration of hydrocarbons in geopressured sediments by buoyancy-driven propagation of methane filled fractures. *American Association of Petroleum Geologists Bulletin* **86**, 907-918.

Nyland, B., Jensen, L.N., Skagen, J., Skarpenes, O., Vorren, T. 1992. Tertiary uplift and erosion in the Barents Sea: Magnitude, timing and consequences. *Norwegian Petroleum Society Special Publication*, **1**, 153-162. Elsevier, Amsterdam.

Paterson, M.S. 1978. *Experimental Rock Deformation: The Brittle Field*. Springer, Berlin.

Pollard, D.D., Segall, P. 1987. Theoretical displacement and stresses near fractures in rocks: with application to faults, points, veins, dikes, and solution surfaces. In: Atkinson, B. (ed.). *Fracture Mechanics of Rocks*. Academic Press, London, 277-349.

Priest, S.D. 1993. *Discontinuity Analysis for Rock Engineering*. Chapman & Hall, London.

Rasmussen, E., Fjeldskaar, W. 1996. Quantification of the Pliocene-Pleistocene erosion of the Barents Sea from present-day bathymetry. *Global and Planetary Change* **12**, 119-133.

Richardsen, G., Vorren, T.O., Torudbakken, B.O. 1993. Post-Early Cretaceous uplift and erosion in the southern Barents Sea; a discussion based on analysis of seismic interval velocities. *Norsk Geologisk Tidsskrift* **73**, 3-20.

Riis, F., Fjeldskaar, W. 1992. On the magnitude of the Late Tertiary and Quaternary erosion and its significance for the uplift of Scandinavia and the Barents Sea. *Norwegian Petroleum Society Special Publication* **1**, 163-185. Elsevier, Amsterdam.

Rohr-Torp, E. 1994. Present uplift rates and groundwater potential in Norwegian hard rocks. *Norges geologiske undersøkelse Bulletin* **426**, 47-52.

Secor, D. T. 1965. The role of fluid pressure in jointing. *American Journal of Science* **263**, 633-646.

Segall, P. 1989. Earthquakes triggered by fluid extraction. *Geology* **17**, 942-946.

Selley, R.C. 1998. *Elements of Petroleum Geology*. Academic Press, London.

Seront, B., Wong, T.-F., Caine, J.S., Forster, C.B., Bruhn, R.L., Fredrich, J.T. 1998. Laboratory characterization of hydromechanical properties of a seismogenic normal fault system. *Journal of Structural Geology* **20**, 865-881.

Shearer, P. 1999. *Introduction to Seismology*. Cambridge University Press, Cambridge.

Sibson, R.H. 1996. Structural permeability of fluid-driven fault-fracture meshes. *Journal of Structural Geology* **18**, 1031-1042.

Sigurdsson, H., Houghton, B., McNutt, S.R., Rymer, H., Stix, J. 2000. *Encyclopedia of volcanoes*. Academic Press, San Diego.

Singhal, B.B.S., Gupta, R.P. 1999. *Applied Hydrogeology of Fractured Rocks*. Kluwer, London.

Sneddon, I. N., Lowengrub, M. 1969. *Crack Problems in the Classical Theory of Elasticity*. Wiley, New York.

Taylor, W.L., Pollard, D.D., Aydin, A., 1999: Fluid flow in discrete joint sets: field observations and numerical simulations. *Journal of Geophysical Research* **104**, 28983-29006.

Tsang, C.F., Neretnieks, I. 1998. Flow channeling in heterogeneous fractured rocks. *Reviews of Geophysics* **36**, 275-298.

Turcotte, D.L., Schubert, G. 2002. *Geodynamics*. 2nd ed. Cambridge University Press, Cambridge.

Twiss, R.J., Moores, E.M. 1992. *Structural Geology*. W.H. Freeman, New York.

Vågnes, E., Faleide. J.I., Gudlaugsson, S.T. 1992. Glacial erosion and tectonic uplift in the Barents Sea. *Norsk Geologisk Tidsskrift* **72**, 333-338.

Valko, P., Economides, M.J. 1995. *Hydraulic Fracture Mechanics*. Wiley, New York.

Vorren, T.O., Richardsen, G., Knutsen, S.M. 1991. Cenozoic erosion and sedimentation in the western Barents Sea. *Marine and Petroleum Geology* **8**, 317-340.

Wood, R.J., Edrich, S.P., Hutchinson, I. 1989. Influence of North Atlantic tectonics on the large-scale uplift of the Stappen High and Loppa High, western Barents Shelf. In: Tankard, A.J., Balkwill, H.R. (eds). Extensional Tectonics and Stratigraphy of the North Atlantic Margins. *American Association of Petroleum Geologists, Memoirs* **46**, 559-566.

Yew, C.H. 1997. *Mechanics of Hydraulic Fracturing*. Gulf Publishing, Houston.

Zoback, M.D., Moos, D., Mastin, L. 1985. Well bore breakouts and in-situ stress. *Journal of Geophysical Research* **90**, 5523-5530.

Zoback, M.L., Zoback, M.D., Adams, J., Assumpcao, M., Bell, S., Bergman, E.A., Bluming, P., Brereton, N.R., Denham, D., Ding, J., Fuchs, K., Gay, N., Gregersen, S., Gupta, H.K., Gvishiani, A., Jacob, K., Klein, R., Knoll, P., Magee, M., Mercier, J.L., Muller, B., Paquin, C., Rajendran, K., Stephansson, O., Suarez, G., Suter, M., Udias, A., Xu, Z.H., Zhizhin, M., 1989: Global Patterns of Tectonic Stress. *Nature* **314**.

Zoback, M.L. 1992. 1st-order and 2nd-order patterns of stresses in the lithosphere - the world stress map project. *Journal of Geophysical Research* **97**, 11703-11728.

Zoback, M.D. 2007. *Reservoir Geomechanics*. Cambridge University Press, Cambridge.